AD NUMBER
AD412677
LIMITATION CHANGES

TO:

Approved for public release; distribution is unlimited. Document partially illegible.

FROM:

Distribution authorized to U.S. Gov't. agencies and their contractors; Administrative/Operational Use; 30 OCT 1961. Other requests shall be referred to Office of Naval Research, Arlington, VA 22203.

AUTHORITY
ONR ltr dtd 4 May 1977

UNCLASSIFIED

AD **412677**

DEFENSE DOCUMENTATION CENTER

FOR

SCIENTIFIC AND TECHNICAL INFORMATION

CAMERON STATION, ALEXANDRIA, VIRGINIA

UNCLASSIFIED

DISCLAIMER NOTICE

THIS DOCUMENT IS THE BEST
QUALITY AVAILABLE.

COPY FURNISHED CONTAINED
A SIGNIFICANT NUMBER OF
PAGES WHICH DO NOT
REPRODUCE LEGIBLY.

G A S L

GENERAL APPLIED SCIENCE LABORATORIES, INC.

STUDIES OF THE
ELECTROMAGNETIC
CHARACTERISTICS OF
MOVING IONIZED GASES
FIRST
SEMIANNUAL TECHNICAL
SUMMARY REPORT

- - - - - - - - - - - - - - - - - - -

GASL TECHNICAL REPORT 255

ARPA Order No. 207-61
Contract No. Nonr 3475 (0 0)
Period: April 1, 1961 to Sept. 30, 1961
Title of Project

"Studies of the Electromagnetic Characteristics of Moving Ionized Gases"

Prepared For

Director
Advanced Research Projects Agency
Department of Defense
The Pentagon
Washington 25, D.C.

Prepared By

General Applied Science Laboratories, Inc.
Merrick and Stewart Avenues
Westbury, L.I., New York

October 30, 1961   Approved By: _____

Antonio Ferri
President

i

TABLE OF CONTENTS

STUDIES OF THE ELECTROMAGNETIC CHARACTERISTICS

OF MOVING IONIZED GASES

The Project Scientist for this task is Dr. Manlio Abele.

The investigations of the microscopic and macroscopic properties in a weakly ionized gas reported in Chapters II and III of this summary report were carried out under the direction of Professors Piero Caldirola and Luigi Napolitano, respectively, and under the general direction of Prof. Piero Caldirola.

The studies of the propagation of electromagnetic waves in the shock tube, reported in Chapter IV, were carried out by Drs. Frank Lane and Gino Moretti.

The experimental work reported in Chapter V has been carried out under the direct supervision of Dr. Abele assisted by Messrs. Roger Tomboulian and Myron Wecker.

CHAPTER I

INTRODUCTION

This report contains preliminary information on the theoretical analysis of the electromagnetic properties of a non-uniform ionized gas and the description of the facility to be used for the experimental investigation of the propagation of an electromagnetic wave in the non-uniform gas.

It is well known that in a first order approximation, the propagation of an electromagnetic wave may be analyzed with a simplified scheme in which the local properties of the ionized gas are given by the plasma frequency and the constant collision frequency. Even in this case the solution of two- or three-dimensional propagation problems may present tremendous mathematical difficulties. On the other hand, in a general case for a non-uniform gas, the effort required to solve these problems is not justified due to the oversimplified scheme of the electrical properties of the gas. When the change of the macroscopic thermodynamic properties of the gas becomes important in a length of the same order of magnitude of a wave length of the electromagnetic field, it becomes necessary to analyze the possible effects of additional phenomena such as the transport process, the anisotropic behavior of the electrical properties, the electrical polarization of the medium, etc. Furthermore, the coupling between transverse oscillations and coherent longitudinal electron oscillations may become a significant factor leading to a substantial increase of the dissipation of electromagnetic energy in

1

thermal energy in the ionized gas. If the relative importance of these phenomena could be properly evaluated from the theoretical standpoint, then it would be possible to define the set of parameters which govern the behavior of an ionized gas for each particular case. The major difficulty of a theoretical approach is due to the fact that it requires detailed information about the microscopic processes, which at the present time is rather incomplete, particularly for the case of weakly ionized air as encountered in flight conditions.

Thus a systematic experimental investigation becomes of primary importance in order to obtain direct information about the electromagnetic properties and it must be complemented by a theoretical analysis of the microscopic processes which occur in a non-uniform gas. Furthermore, a theoretical research has to be developed in order to establish the correlations between the experimental data and the results of the theoretical analysis of the physical properties of the gas.

The experimental investigation of the local electromagnetic properties of a non-uniform gas by means of the study of the propagation of an electromagnetic wave involves a huge amount of difficulties. An overall measurement of the total phase shift and attenuation of the wave across the gas in a given direction would not provide enough information about the local properties. On the other hand, a direct measurement of the distribution of electromagnetic field must be obtained without perturbing both the flow field and the electromagnetic wave. Consequently, the geometry of the channel where

the propagation is analyzed, must be such that the necessary information may be obtained from a set of measurements performed at the boundary of the channel itself. In the case of a one-dimensional non-uniform flow, these considerations suggest the advantage of using the channel containing the ionized gas as an element of wave guide where certain basic conditions about the distribution of the electromagnetic field may be predicted provided that the proper range of frequencies is selected for the electromagnetic field. By using a shock tube to produce the ionized gas, the most simple experimental arrangement corresponds to the propagation of the electromagnetic wave in a section of the driven part of the shock tube itself. A non-uniform distribution of the electrical properties of the gas may be achieved by establishing a temperature gradient in the driven section, as discussed in detail in Chapter V of this report. If the flow were uniform in a cross-section of the wave guide, with a suitable distribution of microwave detectors located at the wall of the wave guide, we would obtain complete information about the properties of propagation of the electromagnetic field. In turn, this information coupled with the theory of propagation in a wave guide leads to the correlation of the measured quantities with the theoretical values of the physical properties of the gas. Of particular interest is the correlation between experimental and theoretical values when the gradient of electron density is chosen in such a way that the electromagnetic wave cannot propagate beyond a given cross-section of the ionized gas. The position of this critical cross-section of the ionized gas and the amount of reflection of the electromagnetic

3

wave at this section should be very sensitive to a small change in the electrical parameters of the gas. Thus we may expect the maximum detectable effect of a departure of the actual physical properties from the theoretical values. This critical cross-section moves along the shock tube with the velocity of the ionized gas. A microwave detector located in the region of propagation before the arrival of the critical cross-section behaves like the detector of a standard standing wave ratio meter. After the instant of time at which the critical cross-section reaches the position of the detector, the detector will indicate the damping of the electromagnetic field in the region of total attenuation.

The position of the initial cross-section may be controlled with an externally applied constant magnetic field. With an axial distribution of magnetic field which should not perturb the gross properties of the flow field, we introduce an additional parameter that may be extremely helpful in obtaining the information about the new properties of propagation which are created in the wave guide. If the microscopic properties of the collision processes in the gas are not strongly affected by the external magnetic field, the anisotropic electrical properties of the ionized gas may be predicted on the basis of the solution of the equations which govern the macroscopic motion of the electrons. A careful analysis of this particular problem from both the microscopic and macroscopic point of view is one of the objectives of the theoretical investigation outlined in this report.

4

The assumption of a one-dimensional flow is verified in the shock tube only in a first order approximation. Actually, the boundary layer behind the shock wave introduces a non-uniform distribution of the electrical properties in a cross-section of the shock tube. The propagation mode chosen for the wave guide is the fundamental T.E. mode, and the frequency of the electromagnetic wave is such that this is the only mode that can be propagated. For these conditions the thickness of the boundary layer where a strong change of the electrical properties may be expected, is a small fraction of the wave length. Consequently, the non-uniform transverse distribution of the flow field will appear as an average effect on the axial propagation of the electromagnetic wave. This effect must be analyzed in order to establish to what extent it may be neglected. A preliminary calculation is presented in this report with a simplified scheme which should give the order of magnitude of the effect to be expected in the experimental conditions of the test section of the shock tube. It is necessary to point out that the boundary layer may introduce additional difficulties corresponding to polarization effects and diffusion processes due to the strong transverse gradients, and a detailed investigation of these effects may become necessary during the development of this research.

On the basis of the aforementioned considerations and the particular experimental technique to be used in the measurement of the electrical properties of the non-uniform flow, the theoretical research program is divided in two main parts. One part is devoted to the analysis of the microscopic

phenomena and the calculations of the parameters which define the physical macroscopic properties of the non-uniform gas. As shown in Chapter II, the statistical approach assumes a weakly ionized gas in such a way that the distribution function for the molecular species is independent of the distribution function for the electron gas. Thus the electric properties of the gas are evaluated in terms of the thermodynamic properties of the non-uniform flow field. This assumption is certainly valid in the particular condition of the gas in the shock tube.

In the other part, the theoretical analysis of the propagation inside the wave guide will be developed with different model distributions of the macroscopic properties of the ionized gas in order to interpret the experimental results and to establish the correlations between the measured electrical properties and the corresponding theoretical values.

6

CHAPTER II

ANALYSIS OF THE MICROSCOPIC PROPERTIES IN A WEAKLY IONIZED GAS

I. INTRODUCTION

The main object of the work presented in this section is to study the effects of inhomogeneities in a plasma caused, for instance, by electric fields, magnetic fields and temperature gradients.

Let us, at first, consider a plasma model without boundary conditions, and assume that the electronic density is much smaller than the molecular density, (Lorentz gas.) In doing so, we may overlook in our model the presence of the ions. Furthermore, if we indicate with $f(P, \underline{v}, t)$ and $F(P, \underline{V}, t)$, respectively, the electronic and molecular distribution functions, we may overlook in the corresponding system of two coupled Boltzmann equations:

$$Df = J_{ee}(f) + J_{em}(f)$$

$$DF = J_{mm}(F) + J_{me}(F)$$

the two collision operators J_{ee} (with respect to J_{em}) and J_{me} (with respect to J_{mm}). A list of symbols is given at the end of this chapter.

Assuming then, the following system for the temporal behavior of f and F,

$$Df = J_{em}(f) \tag{1.1}$$

$$DF = J_{mm}(F), \tag{1.2}$$

we may note that:

a. From the equation (1.2) the temporal behavior of the molecules is entirely independent of the presence of electrons, while the electron gas depends upon the presence of molecules, through the collision term $J_{em}.$

b. The temporal behavior of the electron gas, given by equation (1.1) is affected by the molecular gas, as we shall see later, only through the following phenomenological parameters: molecular density, mean velocity, and mean square velocity.

As a result, it is not necessary in solving equation (1.1) to integrate the Boltzmann equation (1.2):

$$DF = J_{mm}(F),$$

because we only need the knowledge of the mentioned phenomenological parameters.

2. ANALYSIS OF THE EQUATION (1.1)

We shall begin by expanding the electronic distribution function $f(P, \underline{v}, t)$ in spherical harmonics, writing:

$$f(P, \underline{v}, t) = \sum_{j=0}^{\infty} \left[a_{jm}(P, v, t) \, C_{jm} + \beta_{jm}(P, v, t) \, S_{jm} \right], \qquad (2.1)$$

$$(0 \leq m < j)$$

where:

$$C_{jm} = v^j \, \Theta_{jm}(\theta) \cos m\phi$$

$$S_{jm} = v^j \, \Theta_{jm}(\theta) \sin m\phi,$$

$\Theta_{jm}(\theta)$ being the associated Legendre functions:

$$\Theta_{jm}(\theta) = \sin^m \theta \, P_j^{(m)}(\cos \theta).$$

We may write the expansion (2.1) in the form:

$$f(\underline{v}) = f_0(v) + \frac{\underline{v}}{v} \cdot \underline{f}_1(v) + \chi(\underline{v}), \qquad (2.2)$$

where f_0 represents the isotropic part of the distribution function f, $\underline{f}_1$ is the coefficient of the first anisotropy and χ is simply the remaining part of expansion (2.1).

8

Introducing (2.1) into the Boltzmann equation (1.1), we obtain a hierarchy of equations, which is easily obtained provided we know the result of the application of the linear collision operator J over each term of the expansion (2.1).

To this end, we may note that the operator J, in an approximation for which one has simply $m/M = 0$ (perfect Lorentz gas), possesses the following properties, for each isotropic function $a(v)$:

$$J(a) = 0$$

$$J(a\, C_{jm}) = -\nu_j\, a\, C_{jm} \qquad\qquad (2.3)$$

$$J(a\, S_{jm}) = -\nu_j\, a\, S_{jm}$$

In the imperfect Lorentz gas scheme, we shall have:

$$J(a) = O_1\left(\frac{m}{M}\right)$$

$$J(a\, C_{jm}) = -\nu_j\, a\, C_{jm}\left[1 + O_2\left(\frac{m}{M}\right)\right] \qquad (2.4)$$

$$J(a\, S_{jm}) = -\nu_j\, a\, S_{jm}\left[1 + O_3\left(\frac{m}{M}\right)\right]$$

where we have used the Landau symbol $O(x)$, meaning a quantity which is simply of the order of x.

The quantity $O_1\left(\frac{m}{M}\right)$ has been calculated by others (Ref. 2) under the hypothesis of a Maxwellian molecular distribution F, obtaining:

$$J(a) = \frac{m}{M}\,\frac{1}{v^2}\,\frac{\partial}{\partial v}\left[\nu_1\, v^3\left(a + \frac{kT}{mv}\,\frac{\partial a}{\partial v}\right)\right]\ . \qquad (2.5)$$

On the other hand, we have proceeded to the evaluation of the quantity $O_1\left(\frac{m}{M}\right)$ keeping an entirely arbitrary (and hence generally anisotropic) molecular distribution. The result of our calculation is given by:

9

$$J(a) = \frac{1}{v^2} \frac{\partial}{\partial v} \left\{ A(v) + B(v) \, \underline{v} \cdot \overline{\underline{V}} + C(v) \, \overset{\bullet}{\underline{v}\underline{v}} : \overline{\underline{V}\underline{V}} \right\} , \tag{2.6}$$

where:

$$A(v) = \frac{m}{M} \, \nu_1 \, v^3 \, a + \nu_1 \, v^3 \, \frac{\overline{V^2}}{3} \frac{\partial a}{\partial v}$$

$$B(v) = \nu_1 \, v \, a \tag{2.7}$$

$$C(v) = \left(\nu_1 - \frac{1}{2} \nu_2\right) \frac{\partial a}{\partial v} + \frac{3}{v^2} \left[\left(\nu_1 - \frac{1}{2}\nu_2\right) v - \frac{1}{6} \frac{\partial \nu_2}{\partial v} v^2 \right] a \, .$$

We have followed Chapman and Cowling's notation, in writing:

$$\overset{\bullet}{\underline{v}\underline{v}} : \overline{\underline{V}\underline{V}} = \sum_{ij=1}^{3} \left(v_i v_j - \frac{1}{3} v^2 \delta_{ij} \right) \overline{V_j V_i} \, ,$$

where ν_1 and ν_2 are the first two relaxation frequencies (Ref. 1):

$$\nu_1(v) = 2\pi N v \int_0^\pi \sin\theta \left[1 - P_1(\cos\theta) \right] \sigma(\theta, v) \, d\theta$$

$$\tag{2.8}$$

$$\nu_2(v) = 2\pi N v \int_0^\pi \sin\theta \left[1 - P_2(\cos\theta) \right] \sigma(\theta, v) \, d\theta \, ,$$

$\sigma\left(\theta, \left|\underline{v} - \underline{V}\right|\right)$ being the differential cross section for electron-molecule

collision, in a frame of reference fixed with one of the two particles.

The determination of $J(aC_{jm})$, $J(aS_{jm})$ has been done disregarding

the O_2, O_3 terms. (We will give a brief account of the method followed in

the derivation of formula (2.6) later in this chapter) Taking into account

that f_0 is an isotropic function and $\frac{\underline{v}}{v} \cdot \underline{f}_1$ is simply a linear combination

with isotropic coefficients of C_{10}, C_{11}, S_{11}, we are now able to calculate

$J(f_0)$, $J\left(\frac{\underline{v}}{v} \cdot \underline{f}_1\right)$. If we perform a further approximation* forgetting the $\chi(\underline{v})$

---

* As is usual in this kind of reasoning, we may evaluate "a posteriori" the
usefulness of this approximation, by calculating explicitly the difference between
the results obtained and those based on the successive approximation, or
"a priori" we may introduce some plausible arguments, like those used by
Davydov (Ref. 3) and Gurevitch (Ref. 4).

in the (2.2), we at last arrive at the following:

$$D f \equiv J(f) = \frac{1}{v^2} \frac{\partial}{\partial v} \left\{ A + B \underline{v} \cdot \overline{\underline{Y}} + C \underline{\dot{v}} : \overline{\underline{VV}} \right\} - \nu_1 \left(\frac{v}{v} \cdot \underline{f}_1 \right) , \quad (2.9)$$

where $A(v)$, $B(v)$ and $C(v)$ are given by (2.7).

Finally, by means of the orthogonality properties of the spherical harmonics functions on the unity sphere, we obtain the following system:

$$\frac{\partial f_0}{\partial t} + \frac{v}{3} \, \mathrm{div}_p \, \underline{f}_1 + \frac{q_0}{3mv^2} \frac{\partial}{\partial v} (v^2 \, \underline{E} \cdot \underline{f}_1) = \frac{m}{M} \frac{1}{v^2} \frac{\partial}{\partial v} \left[\nu_1 v^3 \left(f_0 + \frac{M\overline{V^2}}{3mv} \frac{\partial f_0}{\partial v} \right) \right]$$

$$(2.10)$$

$$\frac{\partial \underline{f}_1}{\partial t} + v \, \mathrm{grad}_p \, f_0 + \frac{q_0}{m} \frac{\partial f_0}{\partial v} \underline{E} + \frac{q_0}{mc} (\underline{H} \wedge \underline{f}_1) = \left[\frac{1}{v^2} \frac{\partial}{\partial v} (\nu_1 v^2 f_0) \right] \overline{\underline{V}} - \nu_1 \underline{f}_1 ,$$

in the unknown functions f_0, $\underline{f}_1$. *

3. DISCUSSION OF THE COLLISION TERM

The collision term:

$$J(a) \equiv \int (a' F' - a F) \, g \, \sigma (\theta, g) \, d\Omega \, d\underline{V} , \qquad g = |\underline{v} - \underline{V}| \qquad (3.1)$$

has been evaluated by noting that in each electron-molecule collision the variation of the modulus v of electron velocity $\underline{v}$, is given by:

$$\underline{v}' - \underline{v} = O \left[\left(\frac{m}{M} \right)^{1/2} \right] \qquad (3.2)$$

As a consequence, the integral operator (3.1) can be put in a differential form following the same technique which is used in the transformation of the Boltzmann elastic collision operator into the Fokker-Planck form (Refs. 5 and 6).

---

* As will be shown later, the main object of our current research consists in the evaluation of stationary or asymptotic solutions of the system (2.10). Simpler systems, in which we may give evidence to particular aspects of inhomogeneities, will be considered.

Let us introduce a suitable (but largely arbitrary) isotropic function $\bar{\Phi}(v)$; according to a general well known rule:

$$\int J(\iota)\,\bar{\Phi}(v)\;dv = \int \left[\bar{\Phi}(v') - \bar{\Phi}(v)\right]\; g\,a\,F\,\sigma\,(\theta, g)\;d\Omega\;dV\;dv\;, \qquad (3.3)$$

Furthermore, retaining only terms of the order of m/M, we have, according to (3.2):

$$\bar{\Phi}(v') - \bar{\Phi}(v) = (v' - v)\,\frac{\partial \bar{\Phi}}{\partial v} + \frac{1}{2}\,(v' - v)^2\,\frac{\partial^2 \bar{\Phi}}{\partial v^2} \qquad (3.4)$$

Inserting (3.4) into (3.3) and integrating by parts, we found:

$$J(a) = \frac{1}{v^2}\,\frac{\partial}{\partial v}\left[-v^2\,\mu\,a + \frac{1}{2}\,\frac{\partial}{\partial v}\,(v^2\lambda\,a)\right]\;, \qquad (3.5)$$

where

$$\mu(v) = \int \sigma\,(\theta, g)\;g\,F\,(v' - v)\;d\Omega\;dV$$
$$\lambda(v) = \int \sigma\,(\theta, g)\;g\,F\,(v' - v)^2\;d\Omega\;dV \qquad \qquad (3.6)$$

In a way consistent with the approximations used, the two preceding functions μ and λ are evaluated at the first order in the quantity m/M.

The rather lengthy calculations are omitted here. Assuming a quite arbitrary molecular distribution function $F(V)$ and inserting the final expressions for μ and λ into (3.5), we obtain the formula (2.6). We note explicitly that, in the hypothesis that the molecular distribution function F be isotropic, formula (2.6) reduces to (2.5) which has been calculated by Chapman and Cowling (Ref. 2).

12

4. CONCLUDING REMARKS

A preliminary investigation of the possibilities of solving the system (2.10) is now in progress, and in this connection, we intend, in the future, to develop the following points: **a.** To first integrate the system (2.10) for particular cases and then, if possible, in general form. This will be carried out in order to evaluate the electromagnetic parameters of the plasma (taking inhomogeneities into account) within the limits of the approximation used through the knowledge of the electronic distribution function; **b.** To evaluate "a posteriori" the usefulness of the approximations used; and **c.** To work out some possible extensions of the theory.

a. Being aware of the noteworthy analytical difficulties of our system (2.10), we intend, as stated before, to analyze it in more simple cases, at least as a first step. For instance, if we take $E = 0$, $H = 0$, $\overline{V} = 0$ and we consider a stationary state, the system (2.10) reduces to one equation only in the isotropic function f_o, which probably can be integrated in closed form. In this case, with the further hypothesis, $T = \text{const.}$, such an equation is separable; stating

$$f_o(P, v) = R(P) U(v) ,$$

we can write the two following equations:

$$U'' + \left(\frac{\phi'}{\phi} + \frac{2}{v} + \frac{mv}{kT}\right) U' + \left(\frac{mv}{kT}\frac{\phi'}{\phi} + \frac{3m}{kT} + \frac{MKv^2}{3kT\phi^2}\right) U = 0$$

$$\nabla^2 R - \frac{1}{N}\text{grad}_P N \cdot \text{grad}_P R - KN^2 R = 0$$

where

$$v_1(Pv) = N(P)\phi(v) , \qquad \underline{f}_1 = -\frac{v}{N\phi}\text{grad}_P f_o .$$

and K is an arbitrary constant corresponding to the separation of variables.

We intend, by solving these equations, to analyze the influence of the sole density gradient on the electromagnetic properties of the plasma. As far as the attack to the system (2.10) in its more general form is concerned, or, at least, with the only hypothesis of time-independence, we may introduce:

i. some possible reductions of the system to special forms which one can hope to integrate in closed form,

ii. we may look for the evaluation of eigenfunctions and eigenvalues of the operator:

$$J(a) = \frac{m}{M} \ \frac{1}{v^2} \ \frac{\partial}{\partial v} \left[\nu \ v^3 \left(a + \frac{M \overline{V^2}}{3\,mv} \ \frac{\partial a}{\partial v} \right) \right] \quad ,$$

to integrate the system by means of expansion processes provided that the existence of a closed spectrum for J can be proven.

iii. a typical iterative process, on expanding f_0, $\underline{f}_1$, formally, in series of some convenient parameters,

iv. finally, we may integrate the system numerically, at least in the simple cases mentioned above.

b. We intend also, to analyze as accurately as possible the validity of the approximations made in the spherical harmonic expansion used for the electronic distribution. To this end, we will eventually try to consider also the effect of the second order anisotropy. Furthermore, within the limits of elastic collisions, we will analyze more precisely, the particular kind of electron-molecule interaction which affects the form of functions $\nu_1(v)$ and $\nu_2(v)$ of Section 2.

14

c. As regards the extension of the theory, we may take into account more than one kind of spherical molecule. The more useful extension, however, concerns the possibility of taking into account also anelastic collision processes (excitation and ionization) and, at least partially, and in the limit of the Lorentzian gas model, the remaining complex electron-molecule interaction phenomena, which are present in the plasma under various physical conditions (recombination, molecular attachment, etc.).

REFERENCES - CHAPTER II

1. Bayet-Delcroix-Denisse, J. Physique et le Radium, 15, 795 (1954).

2. Chapman, Cowling, The Mathematical Theory of Nonuniform Gases, Cambridge (195.).

3. Davydov, Phys. Zetschriff der Sow, 12, 269, (1937).

4. Gurevitch, A. V. Soviet Physics, JETP, 3, 895 (1957).

5. Uhlenbech, Wang, Rev. Mod. Phys., 17, 323, (1945).

6. Allis, Hand. Der Phys., Springer, New York, 21, (1955).

LIST OF SYMBOLS - CHAPTER II

c = light velocity in vacuum

k = Boltzmann's constant

m = electron mass

q_0 = electron charge

f, F = distribution functions

$\underline{v}$ = electron velocity

v = modulus of electron velocity $(v = |\underline{v}|)$

M = molecular mass

T = molecular temperature

V = modulus of the molecular velocity $(V = |\underline{V}|)$

$\underline{V}$ = molecular velocity

$\overline{\underline{V}}$ = molecular mean velocity

$\overline{V^2}$ = molecular mean square velocity

$\underline{E}$ = electric field

$\underline{H}$ = magnetic field

Df = Boltzmann differential operator for electrons:

$$Df = \frac{\partial f}{\partial t} + \underline{v} \cdot \mathrm{grad}_P f + \frac{q_0}{m} \left(\underline{E} + \frac{1}{c} \underline{v} \wedge \underline{H} \right) \cdot \mathrm{grad}_{\underline{v}} f \ .$$

DF = Boltzmann differential operator for molecules:

$$DF = \frac{\partial F}{\partial t} + \underline{V} \cdot \mathrm{grad}_P F + \frac{X}{M} \cdot \mathrm{grad}_{\underline{V}} F \ .$$

$\underline{X}$ = external forces on molecules

16

$J_{ee}(f)$ = Boltzmann collision operator for electron-electron-encounters

$$J_{ee}(f) = \int b\, d\, b\, d\epsilon \left|\underline{v}' - \underline{v}\right| (f'f_1' - f\, f_1)\, d\underline{v}_1$$

$J_{mm}(F)$ = Boltzmann collision operators for molecule-molecule encounters

$$J_{mm}(F) = \int b\, d\, b\, d\epsilon \left|\underline{V}' - \underline{V}\right| (F'\, F_1' - F\, F_1)\, d\underline{V}_1$$

$J_{em}(f)$ = Boltzmann collision operator for electron-molecule encounters

$$J_{em}(f) = \int b\, d\, b\, d\epsilon \left|\underline{v} - \underline{V}\right| (f'F' - fF)\, d\underline{V}$$

$J_{me}(F)$ = Boltzmann collision operator for molecule-electron encounters

$$J_{me}(F) = \int \mathbf{b}\, d\, b\, d\epsilon \left|\underline{V} - \underline{v}\right| (f'F' - fF)\, d\underline{v} \ .$$

CHAPTER III

MACROSCOPIC PROPERTIES

1.   INTRODUCTION

For this chapter the preliminary results of the study of the electro-magnetic properties of a nonuniform, macroscopically neutral plasma are reported.

The line of approach is a macroscopic one, based on the thermodynamics of irreversible processes. A three-fluid model of the plasma is assumed and, in this first stage, the plasma is considered to be at rest in a suitable reference frame, the components are in mutual thermal equilibrium and imposed magnetic fields are absent. The nonuniformities are those connected with the presence of gradients of state parameters such as temperature, pressure and concentrations.

The presence of these gradients induces a polarization in the medium even in the absence of external electric fields. It will be shown that, in the stationary state, the induced polarization depends on only two independent gradients, which, for convenience, are taken to be those of the temperature and the pressure. An expression for the induced polarization is derived, which is valid for a most general case and which is later simplified to the case of the imperfect Lorentz gas (i.e. weakly ionized plasma for which the mass ratio ξ between the negative charge carriers and neutral molecules is much smaller than one) and the perfect Lorentz gas (i.e. weakly ionized plasma with $\xi = 0$).

18

The phenomenological coefficients relating the induced polarization to the temperature and pressure gradients are first expressed in terms of thermodynamic properties of the plasma. It is then shown how these coefficients can be expressed only in terms of simple binary diffusion coefficients and thermal diffusion coefficients pertinent to the plasma constituents. This last step furnishes the linking element between the present macroscopic approach and the more refined, but usually less general, statistical approach. Indeed it indicates how the subject phenomenological coefficients can be rigorously evaluated, in terms of the "microscopic" characteristics of the plasma constituents, once the statistical approach has gone far enough to provide workable results. In the meantime, however, the fact that one needs to know only the binary transport coefficients provides a possibility of readily performing order of magnitude analysis by utilizing the available experimental data on electron-ions, electron-molecules and ion-molecules collisions.

The results of the present stage of the analysis already open up two possible ways of utilization, both of noticeable interest.

In the first place, as mentioned before, several order-of-magnitude comparative analyses can be carried out. For instance, one can evaluate the relative importance of the different inhomogeneities with respect to the polarizations they are able to induce (e.g., is a temperature or a pressure gradient more important to this effect?) Also, one can compare the polarization induced by the inhomogeneities with that induced by an external electric

field and thus determine the ranges within which the former one can be neglected and the medium treated as homogeneous.

The second application of equal practical interest follows from the consideration of the electromagnetic field which is created by the induced polarization (which, in principle, can be computed by evaluating the Hertz potential whose source is the induced polarization) . When we induce into the plasma a polarization by means of controlled suitable inhomogeneities, part of the energy furnished to maintain the gradients is spent to "create" the induced electromagnetic field. This is nothing but the underlying idea of energy conversion systems and the present results can be used to investigate both the feasibility and efficiency of a number of such systems.

The steps of the analysis herein reported are as follows:

In Section 2 the irreversible thermodynamic description of the system is performed. The extensive and intensive state parameters and the pertinent mass and energy fluxes for a mixture of three fluids, of which two have negative and positive charges, are defined. The "kinetic" relations between fluxes and generalized forces are established and, through suitable use of the basic theorems of the thermodynamics of irreversible processes, the general expression for the mass fluxes in terms of pressure, temperature, the electric potential (ϕ) gradients and thermodynamic properties of the plasma is arrived at.

In Section 3 the general expression for the polarization is obtained, for a macroscopically neutral plasma, in the form:

$$\text{grad } \phi = a_1 \text{ grad } T + a_2 \text{ grad } p$$

where the a_i are phenomenological coefficients. Their expression in terms of the thermodynamic properties of the plasma is also derived in this section, both for the general case and for the simplified case of the Lorentz gas.

In the last section, Section 4, the problem of relating the coefficients a_i to binary transport coeficient is considered. By suitable transformation of fluxes and affinities it is shown how they can be expressed in terms of three binary diffusion coefficients D_{12}, D_{23}, D_{13} and two thermal diffusion coefficients, D_1^T, D_2^T, which refer to the plasma constituents. General expressions are presented but no attempt is yet made to either simplify them or evaluate their comparative order of magnitude.

The concluding section briefly describes the lines along which the research will be furthered

21

2. IRREVERSIBLE THERMODYNAMICS DESCRIPTION OF THE MEDIUM

Considering a plasma formed by electrons (subscript 1), ions (2) and neutral molecules (3) in neutral thermal equilibrium (i.e. $T_1 = T_2 = T_3 = T$) one can write the mass fluxes for the three species and the energy flux as a linear combination of generalized forces (affinities) through phenomenological coefficients. The plasma is assumed to be at rest in a suitable reference frame).

As a consequence of the mass conservation, only two mass fluxes are independent so that, by accounting for the Onsager's principle of the symmetry of the phenomenological coefficients ($L_{ij} = L_{ji}$); one can write:

$$J_o = \sum_{i=1}^{2} Q_i J_i + \left(L_{oo} - \sum_{i=1}^{2} L_{io} Q_i \right) X_o$$

$$(2.1)$$

$$J_i = \sum_{k=1}^{2} L_{ik} \left(X_k - X_3 + Q_k X_o \right) \qquad (i = 1, 2)$$

In these relations J_o is the flux of energy, J_i's are the mass fluxes, and the X_i's are the generalized forces:

$$X_o = - \frac{1}{T} \ \text{grad} \ T$$

$$X_1 = -e_1 \ \text{grad} \ \phi - T \ \text{grad} \left(\frac{\mu_1}{T} \right)$$

$$(2.2)$$

$$X_2 = - e_2 \ \text{grad} \ \phi - T \ \text{grad} \left(\frac{\mu_2}{T} \right)$$

$$X_3 = -T \ \text{grad} \left(\frac{\mu_3}{T} \right)$$

22

with μ_i = specific chemical potential for the ith species, e_i the electric charge per unit mass and ϕ the electric potential.

The quantities Q_i (i = 1, 2) are the heats of transfer, defined in terms of the coefficients L_{ij} as:

$$Q_1 = \frac{L_{10} L_{22} - L_{12} L_{20}}{L_{11} L_{22} - L_{12}^2}$$

(2.3)

$$Q_2 = \frac{L_{11} L_{20} - L_{10} L_{21}}{L_{11} L_{22} - L_{12}^2}$$

It is convenient to eliminate from Equations (2.1) the explicit appearance of the gradients of the chemical potentials μ_k in favor of the pressure gradient. This can be done by considering the $\mu_k = \mu_k(T, p, c_i)$, where c_i is the mass concentration of the ith species, and by taking into due account the definition of Gibb's potential (Reference 2) and the Maxwell's relations (Reference 2).

The result is:

$$J_i = \sum_{k=1}^{2} L_{ik} \left\{ (v_3 - v_k) \ \text{grad} \ p - \sum_{j=1}^{n-1} \left[\left(\frac{\partial (\mu_k - \mu_3)}{\partial c_j} \right)_{p,T,c_k} \cdot \text{grad} \ c_j \right] + \right.$$

(2.4)

$$\left. - (Q_k - h_k + h_3) \ \frac{1}{T} \ \text{grad} \ T \right\} - e_i \ \text{grad} \ \phi$$

$$i = (1, 2)$$

23

where v_i and h_i are the specific volume and enthalpy of the ith component and where the subscripts indicate the variables to be kept constant in the differentiation process.

Equations (2.4) are the equations needed to determine the polarization induced by the inhomogeneities in the plasma, as detailed in the next section.

3.   GENERAL EXPRESSIONS FOR THE POLARIZATION

We are concerned with the determination of the polarization (grad ϕ) induced in the plasma by imposed gradients. We deal, therefore, with a stationary state (Reference 1) wherein all the mass fluxes will be zero while the energy flux J_o is different from zero.

Equations (2.4) equated to zero, plus the statements of mass conservation and macroscopic electrical neutrality provide a set of four equations for the six quantities grad c_i ($i = 1, 2, 3$), grad T, grad p and grad ϕ. It follows that any of these quantities can be expressed as functions of two others.

By choosing the two independent gradients to be the pressure and temperature gradients, one thus obtains the following general expression for the polarization:

$$grad \, \phi = a_1 \, grad \, T + a_2 \, grad \, p. \qquad (3.1)$$

The coefficients a_1 and a_2 are herein referred to as coefficients of polarizability. They are a measure of the polarization induced by the presence of gradients of macroscopic properties of the plasma and are expressed in terms of their thermodynamic properties by:

24

$$a_1 = \frac{q_1\left(\dfrac{b_2}{e_2} - \dfrac{a_2}{e_1}\right) + q_2\left(\dfrac{a_1}{e_1} - \dfrac{b_1}{e_2}\right)}{e_1 e_2\left(\dfrac{a_2 + b_1}{e_1 e_2} - \dfrac{b_2}{e_2^2} - \dfrac{a_1}{e_1^2}\right)}$$

(3.2)

$$a_2 = \frac{\widetilde{m}_1\left(\dfrac{b_2^2}{e_2} - \dfrac{a_2^2}{e_1}\right) + \widetilde{m}_2\left(\dfrac{a_1}{e_1} - \dfrac{b_1}{e_2}\right)}{e_1 e_2\left(\dfrac{a_2 + b_1}{e_1 e_2} - \dfrac{b_2}{e_2^2} - \dfrac{a_1}{e_1^2}\right)}$$

with:

$$a_i = \partial(\mu_i - \mu_3) \,/\, \partial c_1$$

$$b_i = \partial(\mu_i - \mu_3) \,/\, \partial c_2$$

(3.3)

$$\widetilde{m}_i = v_i - v_3 \qquad (i = 1, 2)$$

$$q_i = \frac{1}{T}(Q_i - h_i + h_3)$$

It appears that the a_i, b_i, $\widetilde{m}_i$ are completely determined once the pertinent "state equations" (Reference 2) of the constituents are given. The quantities q_i depend, in addition, upon the phenomenological coefficients L_{ij} through the heats of transfer Q_i.

Thus, to make any use of Equation (3.2) one must make some assumptions as to the state equations of the plasma constituents and must determine, either experimentally or by means of statistical mechanics, the phenomenological coefficients L_{ij}.

The expressions for a_i, b_i and $\widetilde{m}_i$ are herein derived on the assumption that the plasma constituents are perfect gases. The quantities q_i will be dealt with in the next section.

If one makes the perfect gas assumption, the following relations hold (Reference 2):

$$\mu_i = \frac{1}{m_i} RT \left[\oint_i (T) + \ln \left(pc_i \frac{m}{m_i} \right) \right]$$

$$v_i = \frac{m_i}{m} \frac{RT}{pc_i}$$

(3.4)

$$h_i = h_{io} + \int_{T_o}^{T} c_{pi} \, dT$$

wherein $\oint_i (T)$ is an arbitrary function of the temperature, m_i is the molar mass of the ith component, m is the molar mass of the mixture, h_o a reference to specific enthalpy, and R the molar gas constant.

With these expressions one has:

$$a_1 = RT \left\{ \frac{1}{c_1 m_1} - \frac{1}{m_1} \left(\frac{m}{m_1} - \frac{m}{m_3} \right) + \frac{1}{c_3 m_3} + \frac{1}{m_3} \left(\frac{m}{m_1} - \frac{m}{m_3} \right) \right\}$$

$$b_1 = a_2 = RT \left\{ \frac{1}{m_2} \left[\frac{m}{m_3} - \frac{m}{m_1} \right] + \frac{1}{c_3 m_3} + \frac{1}{m_3} \left[\frac{m}{m_3} - \frac{m}{m_1} \right] \right\}$$

(3.5)

$$b_2 = RT \left\{ \frac{1}{c_2 m_2} - \frac{1}{m_2} \left[\frac{m}{m_2} - \frac{m}{m_3} \right] + \frac{1}{c_3 m_3} + \frac{1}{m_3} \left[\frac{m}{m_2} - \frac{m}{m_3} \right] \right\}$$

$$\widetilde{m}_1 = \frac{RT}{pm} \left(\frac{m_1}{c_1} - \frac{m_3}{c_3} \right)$$

$$\widetilde{m}_2 = \frac{RT}{pm} \left(\frac{m_2}{c_2} - \frac{m_3}{c_3} \right)$$

In the case of an imperfect Lorentz gas (i.e. $\frac{m_1}{m_3} << 1$; $N_1/N_3 << 1$; $N_2/N_3 << 1$) these formulae are greatly simplified and one obtains:

$$\frac{a_1}{e_1} \simeq \frac{NRT}{\epsilon_1} \quad \frac{m}{m_1}$$

$$b_1 = a_2 \simeq 0$$

$$\frac{b_2}{e_2} \simeq \frac{NRT}{\epsilon_2} \quad \frac{m}{m_2} \tag{3.6}$$

$$\widetilde{m}_i = \frac{RT}{pm} \quad \frac{m_i}{c_i}$$

where ϵ_1 and ϵ_2 are the molar electric charges.

The expressions for the coefficients a_1 and a_2 are found by substituting Equations (3.5) into Equations (3.2).

Another quantity of practical interest is the coefficient $a_3 = a_2/a_1$, giving a measure of the relative importance of pressure and temperature gradients with respect to the induction of polarization.

The general expression for a_3 is:

$$a_3 = \frac{\widetilde{m}_1 + \widetilde{m}_2 \, \theta}{q_1 + q_2 \, \theta} \tag{3.7}$$

where

$$\theta = \frac{\dfrac{a_1}{e_1} - \dfrac{b_1}{e_2}}{\dfrac{b_2}{e_2} - \dfrac{a_2}{e_1}} \tag{3.8}$$

In the case of imperfect Lorentz's gas, Equation (3.7) reduces to:

$$a_3 = \frac{RT}{pm} \left[\frac{m_2}{c_2} \frac{\epsilon_2}{\epsilon_1} \frac{m_2}{m_1} \right] \bigg/ \left[q_1 + q_2 \frac{\epsilon_2}{\epsilon_1} \frac{m_2}{m_1} \right] \qquad (3.9)$$

$$a_1 \simeq Nm \left(q_1 \frac{1}{\epsilon_2 m_2} + q_2 \frac{1}{\epsilon_1 m_1} \right) \bigg/ \left(\frac{\epsilon_1}{\epsilon_2} \frac{1}{m_2 c_1} + \frac{\epsilon_2}{\epsilon_1} \frac{1}{c_2 m_1} \right) \qquad (3.10)$$

The formulae so far developed are all that one can do without specifying the nature of the phenomenological coefficients L_{ij}. Any order of magnitude analysis can be furthered only after having found suitable expressions for these coefficients, or, what amounts to the same, for the quantities q_i.

This is considered in the next section, where it will be shown how the L_{ij}'s can all be expressed in terms of binary transport coefficients.

4.   EXPRESSIONS OF THE PERTINENT PHENOMENOLOGICAL COEFFICIENTS

   IN TERMS OF BINARY TRANSPORT COEFFICIENT

To express the coefficients q_i in terms of binary transport coefficients the following consideration is essential.

In the subject case we have two independent mass fluxes and one energy flux. The number of independent phenomenological coefficients is therefore, accounting for the three Onsager's relations between the six cross-coefficients, six. It follows that the behavior of the system is completely characterized by only six independent coefficients. A set of six independent coefficients is that of the three binary diffusion coefficients D_{12}, D_{13}, D_{23} (i.e. the coefficients of diffusion for electrons -ions, electrons-molecules, and ions-molecules mixtures) plus the two binary thermal diffusion coefficients D_1^T, D_2^T (i.e. the coefficients

28

of thermal transport due to diffusion of the electron-gas and the ion-gas into the neutral gas, respectively) and the heat conduction coefficient.

It is then natural to think that a suitable linear transformation of fluxes and forces will make it possible to express everything in terms of the above binary transport coefficients.

This is indeed so. In fact, by defining the new fluxes J_k' and forces X_k' through the relations:

$$
\begin{aligned}
J_i' &= J_1 && (i = 1, 2, 3) \\
J_o' &= J_o - h_1 J_1 - h_2 J_2 - h_3 J_3 && (4.1) \\
X_i' &= X_i + h_i X_o \\
X_o' &= X_o
\end{aligned}
$$

We find (see Reference 2) the following relations between the coefficients L_{ij} and the new coefficients L_{ij}'.

$$
\begin{aligned}
L_{ij}' &= L_{ij} && (i, j = 1, 2, 3) \\
L_{oo}' &= L_{oo} && (4.2) \\
L_{1o}' &= -L_{11}(h_1 - h_3) - L_{12}(h_2 - h_3) + L_{1o} \\
L_{2o}' &= -L_{21}(h_1 - h_3) - L_{22}(h_2 - h_3) + L_{2o}
\end{aligned}
$$

These new coefficients L_{ij}' are just those used in Reference 3 and it is therein shown how they are related to the binary diffusion coefficients D_{ij}, to the thermal diffusion coefficients D_i^T (i = 1, 2) and to the thermal conductivity coefficient h'.

29

By performing the necessary substitutions, the ultimate goal of expressing the q_i's in terms of binary transport coefficients is thus achieved, and one obtains:

$$q_1 = -\frac{1}{AT}\left\{ n^2 n_1 n_2 m_1 m_2 \left[n_3 m_3^2 D_{13} D_{23} + m_2 (\rho = n_2 m_2) D_{12} D_{23} \right. \right.$$

$$\left. - m_1 (\rho - n_1 m_1) D_{12} D_{13}\right] \left[D_1^T + D_2^T \right] + (D_1^T) n^2 n_2 n_3 m_2 m_3 \left[n_1 m_1^2 D_{21} D_{31} + \right.$$

$$\left. \left. - m_3 (\rho - n_3 m_3) D_{23} D_{31} - m_2 (\rho - n_2 m_2) D_{23} D_{21} \right] \right\} \qquad (4.3)$$

and

$$q_2 = -\frac{1}{AT}\left\{ n^2 n_1 n_2 m_1 m_2 \left[n_3 m_3^2 D_{13} D_{23} - m_2 (\rho - n_2 m_2) D_{12} D_{23} \right. \right.$$

$$\left. - m_1 (\rho - n_1 m_1) D_{12} D_{13}\right] \left[D_1^T + D_2^T \right] + (D_2^T) \left[n^2 n_1 n_3 m_1 m_3 \right] \cdot$$

$$\cdot \left[n_2 m^2 D_{12} D_{32} - m_3 (\rho - n_3 m_3) D_{13} D_{32} - m_1 (\rho - n_1 m_1) D_{13} D_{12} \right] \right\}$$

where A is given by:

$$A = \left[\rho^2 p (n_1 D_{23} + n_2 D_{13} + n_3 D_{12}) \right]^{-1} \cdot \left\{ n^2 n_1 n_3 m_1 m_3 \left[n_2 m_2^2 D_{12} D_{32} + \right. \right.$$

$$\left. - m_3 (\rho - n_3 m_3) D_{13} D_{32} - m_1 (\rho - n_1 m_1) D_{13} D_{12}\right] n^2 n_1 n_2 m_1 m_2 \quad \cdot$$

$$\left[n_3 m_3^2 D_{13} D_{23} - m_2 (\rho - n_2 m_2) D_{12} D_{23} - m_1 (\rho - n_1 m_1) D_{12} D_{13}\right] +$$

$$n^2 n_1 n_3 m_1 m_3 \left[n_2 m_2^2 D_{12} D_{32} - m_3 (\rho - n_3 m_3) D_{13} D_{32} - m_1 (\rho - n_1 m_1) \right. \quad \cdot$$

$$\cdot D_{13} D_{12} \right] n^2 n_2 n_3 m_2 m_3 \left[n_1 m_1^2 D_{21} D_{31} - m_3 (\rho - n_3 m_3) D_{23} D_{31} + \right.$$

$$\left. - m_2 (\rho - n_2 m_2) D_{23} D_{21} \right] + n^2 n_1 n_2 m_1 m_2 \left[n_3 m_3^2 D_{13} D_{23} - m_2 (\rho - n_2 m_2) \right. \quad \cdot$$

$$\cdot D_{12} D_{23} - m_1 (\rho - n_1 m_1) D_{13} D_{12} \bigg] n^2 n_2 n_3 m_2 m_3 \bigg[n_1 m_1^2 D_{21} D_{31} +$$

$$-m_3 (\rho - n_3 m_3) D_{23} D_{31} - m_2 (\rho - n_2 m_2) D_{23} D_{21} \bigg] \bigg\}$$

At this point the new polarization coefficients result expressed as functions of D_{i_j} and D_i^T only. One could carry the analysis further and relate them to the appropriate integrals of the distribution functions for the three constituents thus establishing the link between the present macroscopic approach and the statistical one. We don't pursue this aspect any further since all the required passages and formulae are developed extensively in Reference 3, (part 2, Chapter 7) to which the reader is referred for details.

5. CONCLUDING REMARKS

The general expression for the polarization induced by inhomogeneities has been herein derived. Two new "polarizability" coefficients α_1 and α_2 have been defined which are a measure of these effects and which have been expressed in terms of the thermodynamic state equations of the plasma constituents and of binary transport coefficients.

In the subsequent stage of the research, an order of magnitude analysis will be performed to determine both the absolute and relative importance of temperature and pressure gradients with respect to the induction of polarization in a plasma. This can be done by a judicious choice of the values of the binary transport coefficients, as they are presently available in the literature on the assumption that the constituent gasses obey perfect-gas state equations.

31

The present method of approach, furthermore, will be extended to include the following effects:

    i)   presence of an imposed magnetic field (i.e. study of a plasma medium which is both nonhomogeneous and anisotropic)

    ii)   plasma constituents not thermally in equilibrium (i.e. electron, ion and neutral gasses with different temperatures)

    iii)   nonuniform convective motion of the plasma.

REFERENCES - CHAPTER III

1.   De Groot, The Thermodynamics of Irreversible Processes, North Holland, 1951.

2.   Callen, Thermodynamics, J. Wiley and Sons, 1960.

3.   Hirshfelder, Curtiss, Bird, Molecular Theory of Gases and Liquids, Wiley and Sons, 1954.

SYMBOLS - CHAPTER III

c_i mass concentration of i component

D_i^T coefficient of thermal diffusion

D_{ij} coefficient of binary molecular diffusion between the species i and j

e_i electric charge per unit mass of the i component

E external electric field

g Gibbs' specific potential

h specific enthalpy

J_i mass flow of i component referred to the baricenter of the mixture

J_o energy flow

m molar mass of the mixture $= \dfrac{\epsilon\, m_i\, N_i}{N}$

n number density of the mixture $= \dfrac{N}{V}$

n_i number density of i component

N_i molar concentration of i component

N molar concentration of the mixture

p pressure

P polarization

s specific entropy

T temperature

u specific internal energy

V specific volume

a_1, a_2 new polarizability coefficients

33

SYMBOLS (Continued)

ϵ molar electric charge

λ' thermal conductivity coefficient

μ electrochemical potential

ρ density

ϕ electric potential

ω angular wave frequency

CHAPTER IV

PROPAGATION OF ELECTROMAGNETIC WAVES IN THE SHOCK TUBE

1. INTRODUCTION

The present part of the theoretical work on the **propagation** of an electromagnetic field in a plasma is connected with the experimental program of measurement of the electrical properties of the plasma in the shock tube.

The test section of the shock tube is used as a section of wave guide in which the phase velocity and the attenuation of the selected mode of propagation will be measured. The propagation constant of the electromagnetic wave depends upon both the axial and radial distribution of the electric properties of the plasma. The axial gradient of electron density is controlled by the temperature distribution in the driven section of the shock tube. On the other hand we may expect a radial nonuniform distribution in the electron density due to the growing thickness of the boundary layer behind the shock wave. The rate of increase of the boundary layer thickness corresponds to **a s**mall change of the radial distribution **inside a wavelength** of the field distribution in the wave guide. Consequently the effects of radial and axial nonuniform distributions can be analyzed independently.

The local value of the phase velocity along the wave guide depends upon some average value of radial electron distribution. This dependence must be analyzed in order to determine the error which may be introduced in the correlation of the experimental results with a propagation model in which the radial distribution is not taken into account.

In order to discuss this effect a theoretical analysis of the propagation

properties is being conducted assuming a circular wave guide of radius r_2 in

which the plasma is contained in a cylinder of radius $r_1 < r_2$. The values of

$r_2 - r_1$ are selected according to the expected thickness of the layer in which

the electron density decays rapidly in the neighborhood of the wall. The step

function distribution is selected in order to obtain the maximum possible effect

of the boundary layer on the axial propagation of the electromagnetic wave. This

problem is analyzed in Section 3 of this chapter. In the final stage of the ex-

perimental program we are planning to measure the propagation properties in

the wave guide also with an axial constant and uniform magnetic field in the

test section of the shock tube. These measurements will provide an additional

set of data on the electromagnetic properties of the plasma. For this reason

a theoretical analysis is being conducted in order to calculate the propagation

properties and in particular to discuss the effect of the magnetic field on the

lowest modes of propagation of the wave guides containing the ionized gas. The

preliminary results of these calculations are contained in the last section of this

chapter.

2.   BASIC EQUATIONS

The mathematical model of Maxwell equations together with an electron

momentum equation is developed first in a general way and then specialized to

the specific problem treated. The plasma is assumed to be defined by a constant

plasma frequency and a constant collision frequency. The system of equations

upon which the analysis is based is as follows:

36

$$\nabla \times \vec{E} = -\dot{\vec{H}} \mu \qquad\qquad (1)$$

$$\nabla \times \vec{H} = \epsilon \dot{\vec{E}} - en\vec{w} \qquad\qquad (2)$$

$$m\dot{\vec{w}} = -\nu m\vec{w} - e\vec{E} - \mu e\vec{w} \times \vec{H}_o \qquad\qquad (3)$$

where $\vec{E}$, $\vec{H}$, are respectively electric and magnetic oscillatory fields and $\vec{H}_o$ is the axial applied (steady) magnetic field, $\vec{w}$ is electron velocity, ν is collision frequency, m is electron mass, (-e) is electron charge, and ϵ, μ are dielectric permeability and magnetic permeability, respectively, for a vacuum. The electrons are assumed to have significant collisions with neutral particles only, and ν is the frequency for this type of collision.

Under harmonic time-dependence $e^{-i\omega t}$ the equations become:

$$\nabla \times \vec{E} = i\omega \mu \vec{H} \qquad\qquad (4)$$

$$\nabla \times \vec{H} = -i\omega \epsilon \vec{E} - en\vec{w} \qquad\qquad\cdot\qquad (5)$$

$$(\nu - i\omega)\ \vec{w} = \frac{-e}{m}\vec{E} - \frac{\mu e}{m}\vec{w} \times \vec{H}_o = -\frac{e}{m}\vec{E} - \vec{w} \times \vec{i}_z\ \omega_H \qquad (6)$$

where $\omega_H = \dfrac{\mu e H_o}{m}$ is (electron) gyro grequency and $\vec{i}_z$ is the unit vector in the axial or z-direction.

It proves convenient to partition both vectors and (curl) operators into axial ( )$_z$ and transverse ( )$_s$ components.

$$\text{Thus} \qquad \vec{E} = \begin{pmatrix} E_r \\ E_\theta \\ 0 \end{pmatrix} + \begin{pmatrix} 0 \\ 0 \\ E_z \end{pmatrix} \quad \text{or} \quad \begin{pmatrix} E_x \\ E_y \\ 0 \end{pmatrix} + \begin{pmatrix} 0 \\ 0 \\ E_z \end{pmatrix} \Bigg\} \ (7)$$

$$= E_s + E_z$$

and similarly with $\vec{H}$.

The curl operator is partitioned in the following manner:

$$\nabla \times \ = \ \begin{vmatrix} i & j & k \\ \dfrac{\partial}{\partial x} & \dfrac{\partial}{\partial y} & 0 \\ (\ ) & (\ ) & (\ ) \end{vmatrix} \ + \ \begin{vmatrix} i & j & k \\ 0 & 0 & \dfrac{\partial}{\partial z} \\ (\ ) & (\ ) & (\ ) \end{vmatrix} \qquad (8)$$

$$= \quad \nabla_s \times (\ ) \quad + \quad \nabla_z \times (\ )$$

where the partitioning is illustrated in Cartesian coordinates for simplicity, z still being considered as axial.

Applying this partitioning to the system (4), (5), (6), the following system results:

$$\nabla_s \times E_s \ = \ i \omega \mu H_z \qquad (9)$$

$$\nabla_s \times E_z \ + \ \nabla_z \times E_s \ = \ i \omega \mu H_s \qquad (10)$$

$$\nabla_s \times H_s \ = \ -i \omega \epsilon E_z - e n w_z \qquad (11)$$

$$\nabla_s \times H_z \ + \ \nabla_z \times H_s \ = \ -i \omega \epsilon E_s - e n w_s \qquad (12)$$

$$(\nu - i \omega) \ w_z \ = \ -\frac{e}{m} E_z \qquad (13)$$

$$(\nu - i \omega) \ w_s \ = \ -\frac{e}{m} E_s \ + \ \omega_H i_z \times w_s \qquad (14)$$

In the above system, Equations (9), (11), (13) are scalar single equations and (10), (12), (14) are vector equation pairs in the (x, y) or (r, θ) plane. The last equation (14) can be solved for the two components, w_r and w_θ, of w_s :

38

$$T \begin{pmatrix} w_r \\ w_\theta \end{pmatrix} = - \frac{e}{m} \cdot \begin{pmatrix} E_r \\ E_\theta \end{pmatrix} \tag{15}$$

or $\qquad w_s = - \frac{e}{m} T^{-1} E_s \tag{16}$

where

$$T = \begin{pmatrix} \nu - i\omega & \omega_H \\ -\omega_H & \nu - i\omega \end{pmatrix} \tag{17}$$

From (14)

$$w_z = \frac{-e}{m(\nu - i\omega)} E_z \tag{18}$$

Substituting from (16) and (18) into (11), (12) for w_z, w_s, there results

$$\nabla_s \times H_s = - i\omega \epsilon E_z + \frac{e^2 n E_z}{m(\nu - i\omega)} = - i\omega \epsilon E_z + \omega_p^2 \frac{\epsilon}{\nu - i\omega} E_z \tag{19}$$

$$= \widetilde{R} E_z$$

where $\omega_p^2 = \dfrac{e^2 n}{\epsilon m}$ is (plasma frequency)^2

$$\nabla_s \times H_z + \nabla_z \times H_s = - i\omega \epsilon E_s + \omega_p^2 \epsilon T^{-1} E_s \tag{20}$$

$$= R E_s$$

where the scalar $\widetilde{R}$ and the matrix R are given by

$$\widetilde{R} = \frac{\omega_p^2 \epsilon}{\nu - i\omega} - i\omega\epsilon \tag{21}$$

$$R = - i\omega \epsilon I + \omega_p^2 \epsilon T^{-1} \tag{22}$$

with I representing the 2 X 2 unit matrix.

39

Now solving formally, (10) for H_s and (20) for E_s, we find

$$H_s = \frac{1}{i\omega\mu} (\nabla_s \times E_z + \nabla_z \times E_s) \qquad (23)$$

$$E_s = R^{-1} (\nabla_s \times H_z + \nabla_z \times H_s) \qquad (24)$$

The objective here is to express the transverse fields, H_s, E_s entirely in terms of the axial components E_z, H_z. This is accomplished by substituting (23) into (24) and (24) into (23).

$$H_s = \frac{1}{i\omega\mu} \left(\nabla_s \times E_z + \nabla_z \times (R^{-1} \nabla_s \times H_z + R^{-1} \nabla_z \times H_s) \right) \qquad (25)$$

$$E_s = R^{-1} \left(\nabla_s \times H_z + \frac{1}{i\omega\mu} \nabla_z \times (\nabla_s \times E_z + \nabla_z \times E_s) \right) \qquad (26)$$

But it can be easily shown that

$$\nabla_z \times \nabla_z \times E_s = -\frac{\partial^2 E_s}{\partial z^2} \qquad (27)$$

and

$$\nabla_z \times (R^{-1} \nabla_z \times H_s) = -R^{-1} \frac{\partial^2 H_s}{\partial z^2} \qquad (28)$$

In the cavity mode problem, only the first axial harmonic is desired. Thus, for the cavity problem the z-dependence of E_z and H_z is given by

$$E_z(r, \theta) \sin \frac{\pi z}{z_o} z \qquad (29)$$

$$H_z(r, \theta) \cos \frac{\pi z}{z_o} \qquad (30)$$

so that

$$\frac{\partial^2 (\ )}{\partial z^2} \quad \frac{-\pi^2 (\ )}{z_o^2} \qquad (31)$$

where z_o is the axial length of the cavity. In the wavequide problem the

z-dependence of E_z and H_z is given by

$$E_z(r, \theta) \; e^{i\tilde{\gamma} z} \tag{32}$$

$$H_z(r, \theta) \; e^{i\tilde{\gamma} z} \tag{33}$$

so that $\quad \dfrac{\partial^2}{\partial z^2} \quad = \; - \tilde{\gamma}^2 \tag{34}$

Hence, in what follows $\partial^2/\partial z^2$ may be replaced by either $- \pi^2/z_o^2$ or $-\tilde{\gamma}^2$ and no confusion should result. This, together with (27) and (28) permits solution of (25) and (26) for E_s, H_s in terms of E_z, H_z.

$$E_s = \left(I - \frac{\pi^2 R^{-1}}{z_o^2 \, i \, \omega \, \mu} \right)^{-1} \; R^{-1} \left(\nabla_s \times H_z + \frac{1}{i \omega \mu} \nabla_z \times \nabla_s \times E_z \right) \tag{35}$$

$$H_s = \left(I - \frac{\pi^2 R^{-1}}{z_o^2 \, i \, \omega \, \mu} \right)^{-1} \; \frac{1}{i \omega \mu} \left(\nabla_s \times E_z + \nabla_z \times (R^{-1} \nabla_s \times H_z) \right) \tag{36}$$

This expresses E_s and H_s in the desired form.

For convenience in subsequent expressions, the following notation is introduced

$$R^{-1} = \begin{pmatrix} \alpha & \beta \\ -\beta & \alpha \end{pmatrix} \tag{37}$$

$$\left(I - \frac{\pi^2 R^{-1}}{z_o^2 \, i \omega \, \mu} \right)^{-1} = \begin{pmatrix} \delta & \gamma \\ -\gamma & \delta \end{pmatrix} \tag{38}$$

Then, if E_s and H_s from (35) and (36) are substituted into (9) and (19), using the α, β, γ, δ notation of (37) and (38), the following two coupled equations for H_z (henceforth called simply H) and E_z (called E) are obtained:

41

$$\widetilde{R} \, i\omega\mu E \; + \; \delta\left(\frac{1}{r}\;\frac{\partial}{\partial r}\;\frac{r\,\partial E}{\partial r}\right) \; + \; \left(\frac{\gamma\alpha + \delta\beta}{r}\right)\;\frac{\partial}{\partial r}\left(\frac{r\,\partial^2 H}{\partial z\,\partial r}\right) \; +$$

$$+ \;\; \frac{\delta}{r^2}\;\;\frac{\partial^2 E}{\partial\theta^2} \;\; + \;\; \frac{\gamma\alpha + \delta\beta}{r^2}\;\;\frac{\partial^3 H}{\partial z\,\partial\theta^2} \;\; = \;\; 0 \tag{39}$$

$$i\omega\mu\, H \; + \; (\delta\alpha - \gamma\beta)\left(\frac{1}{r}\;\frac{\partial}{\partial r}\left(r\,\frac{\partial H}{\partial r}\right)\right) \; + \left(\frac{1}{r^2}\;\frac{\partial^2 H}{\partial\theta^2}\right)$$

$$+ \;\; \frac{\gamma\alpha + \delta\beta}{i\omega\mu}\left[\frac{1}{r}\;\;\frac{\partial}{\partial r}\;\;\left(r\,\frac{\partial^2 E}{\partial r\,\partial z}\right) \; + \; \frac{1}{r^2}\;\;\frac{\partial^3 E}{\partial z\,\partial\theta^2}\right] \;\; = \;\; 0 \tag{40}$$

Letting the θ-dependence be given by $e^{im\theta}$ in all cases, and using the operator notation

$$L_m \;\; = \;\; \frac{1}{r}\;\frac{\partial}{\partial r}\;\left(r\,\frac{\partial}{\partial r}\right) \; - \; \frac{m^2}{r^2} \tag{41}$$

the equations (39) and (40) reduce to

$$\widetilde{R} \, r\omega\mu E \; + \; \delta L_m E \; + \;\; \frac{\pi}{z_0}\;(\gamma\alpha + \delta\beta)\; L_m H \; = \;\; 0 \tag{42}$$

$$i\omega\mu\, H \; + \; (\delta\alpha - \gamma\beta)\; L_m H \; - \; \frac{\pi}{z_0}\;\left(\frac{\gamma\alpha + \delta\beta}{i\omega\mu}\right)\; L_m E \; = \; 0 \tag{43}$$

Eliminating H by cross operating on these equations, we find

$$a\,L_m^2\, E \; + \; b\,L_m E \; + \; cE \; = \;\; 0 \tag{44}$$

with

$$a \;\; = \;\; \frac{\pi^2}{z_0^2}\;\;\frac{(\gamma\alpha + \delta\beta)^2}{(i\omega\mu)^2} \;\; + \;\; (\delta\alpha - \gamma\beta)\;\;\frac{\delta}{i\omega\mu} \tag{45}$$

42

$$b = \delta + \widetilde{R}(\delta a - \gamma\beta) \tag{46}$$

$$c = \widetilde{R}\,i\omega\mu \tag{47}$$

This has the solutions $J_m(rk_1)$, $J_m(rk_2)$, $Y_m(rk_1)$, $Y_m(rk_2)$

where

$$k_{\genfrac{}{}{0pt}{}{1}{2}} = \sqrt{\frac{b \pm \sqrt{b^2 - 4ac}}{2a}} \tag{48}$$

. Incidentally, H can be shown to satisfy the same equation (44) and hence to have solutions composed of the same functions.

The combinations of a, β, γ, δ required are as follows for the case of zero collision frequency ($\nu = 0$).

$$a = \frac{\left(\dfrac{\omega_H^2 - \omega^2}{\epsilon}\right) i\omega\,(\omega^2 - \omega_p^2 - \omega_H^2)}{-\omega^2(\omega^2 - \omega_p^2 - \omega_H^2)^2 + \omega_H^2\,\omega_p^2}$$

$$\beta = \frac{\left(\dfrac{\omega_H^2 - \omega^2}{\epsilon}\right)\omega_H\omega_p^2}{-\omega^2(\omega^2 - \omega_p^2 - \omega_H^2)^2 + \omega_H^2\,\omega_p^2}$$
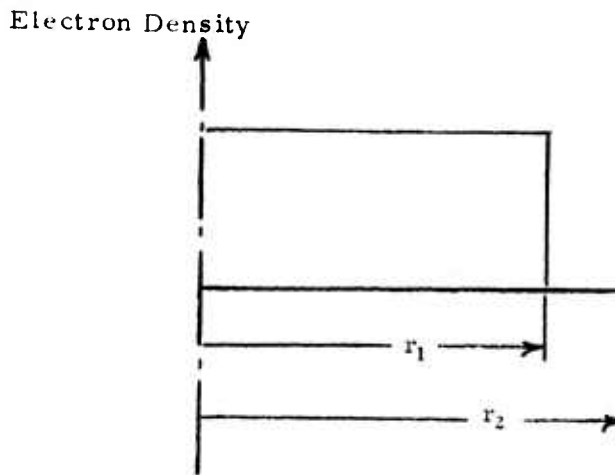
$$\delta = \frac{\left(1 - \dfrac{\pi^2 a}{z_o^2\,i\omega\mu}\right)}{\left(1 - \dfrac{\pi^2 a}{z_o^2 i\omega\mu}\right)^2 + \left(\dfrac{\pi^2\beta}{z_o^2 i\omega\mu}\right)^2}$$

$$(\gamma a + \delta\beta) = \frac{\beta}{\left(1 - \dfrac{\pi^2 a}{z_o^2 i\omega\mu}\right)^2 + \left(\dfrac{\pi^2\beta}{z_o^2 i\omega\mu}\right)^2}$$

$$\tag{49}$$

$$(\delta\alpha - \gamma\beta) = \left(\frac{\alpha - \dfrac{\pi^2(\alpha^2 + \beta^2)}{z_o^2 \, i\omega\mu}}{\left(1 - \dfrac{\pi^2\alpha}{z_o^2 \, i\omega\mu}\right)^2 + \left(\dfrac{\pi^2\beta}{z_o^2 \, i\omega\mu}\right)^2} \right)$$

Note that β and $(\gamma\alpha + \delta\beta)$ vanish with the magnetic field (i.e. as $\omega_H \to 0$).

44

3. PROPAGATION OF AN ELECTROMAGNETIC WAVE IN A CIRCULAR WAVEGUIDE WITH A PIECEWISE CONSTANT RADIAL ELECTRON DENSITY DISTRIBUTION

Electron Density

The sketch shows the radial variation of electron density considered in the wave propagation analysis. As noted earlier, this is intended to simulate the rapid radial decay of electron density in the boundary layer. For this problem, no externally applied steady magnetic field is considered. The uncoupling realized in the cavity mode problem by the disappearance of applied magnetic field does not carry through to the present problem (except for θ-independent waves) due to the radial nonuniformity of the plasma electron density.

However, with the disappearance of ω_H, the matrices T, R, etc., degenerate to simple scaler quantities. Thus

$$R \quad \text{becomes} \quad \epsilon \left(\frac{\omega_p^2}{\nu - i\omega} - i\omega \right) \tag{50}$$

$$\left(I - \frac{\pi^2}{z_0^2} \frac{R^{-1}}{i\omega\mu} \right) \quad \text{becomes} \quad \left[1 - \frac{\tilde{\gamma}^2}{i\omega\mu\epsilon \left(\frac{\omega_p^2}{\nu - i\omega} - i\omega \right)} \right] \tag{51}$$

45

Hence

β , γ become zero

and δ becomes

$$\frac{1}{1 - \dfrac{\tilde{\gamma}^2}{i\omega\mu\,\epsilon\left(\dfrac{\omega_p^2}{\nu - i\omega} - i\omega\right)}} = \frac{k_o^2 + \dfrac{i\omega\mu\,\epsilon\,\omega_p^2}{\nu - i\omega}}{k_o^2 - \tilde{\gamma}^2 + \dfrac{i\omega\mu\,\epsilon\,\omega_p^2}{\nu - i\omega}} \tag{52}$$

while α

becomes

$$\frac{1}{\epsilon\left(\dfrac{\omega_p^2}{\nu - i\omega} - i\omega\right)} \tag{53}$$

In the above expressions (50) through (53) the value of ω_p^2 is to be taken as ω_p^2 in the plasma and zero in the vacuum annulus.

With the vanishing of β and γ, equations (42) and (43) uncouple, and both E and H satisfy a reduced wave equation of the form

$$\frac{1}{r}\,\frac{\partial}{\partial r}\left(r\,\frac{\partial u}{\partial r}\right) - \frac{m^2}{r^2}\,u + \left(k_o^2 - \tilde{\gamma}^2 + \frac{i\omega\omega_p^2}{c^2(\nu - i\omega)}\right) u = 0 \tag{54}$$

u representing E or H.

These have the solutions

$$u = \left\{ \begin{array}{l} J_m\left(k_o r\,\sqrt{1 - \dfrac{\omega_p^2\left(1 - \dfrac{i\nu}{\omega}\right)}{\omega^2 + \nu^2} - \dfrac{\tilde{\gamma}^2}{k_o^2}}\right) \\[4mm] Y_m\left(k_o r\,\sqrt{1 - \dfrac{\omega_p^2\left(1 - \dfrac{i\nu}{\omega}\right)}{\omega^2 + \nu^2} - \dfrac{\tilde{\gamma}^2}{k_o^2}}\right) \end{array} \right. \tag{55}$$

In the outer vacuum annulus, both solutions (55) must be used (for both E and H) with $\omega_p = 0$. In the inner plasma-filled cylinder, only the J_m contributions apply, from boundedness considerations. This leaves three undetermined coefficients for each of E and H. Correspondingly, there are two boundary conditions:

$$E(r_2) = 0$$

$$E_{(\theta)}(r_2) = 0 \tag{56}$$

46

and four interface or jump conditions at $r = r_1$.

$$[E] = 0$$

$$[E_{(\theta)}] = 0$$

$$[H] = 0 \tag{57}$$

$$[H_{(\theta)}] = 0$$

In (57) the **sym**bol $[\;]$ means jump in a quantity across $r = r_1$.

The jump conditions (57) on $E_{(\theta)}$ and $H_{(\theta)}$ require expression of these quantities in terms of E and H. From equations (35) and (36) and the scalar nature of R (50), the expressions for $E_{(\theta)}$ and $H_{(\theta)}$ can be written as follows:

$$E_{(\theta)} = -\delta a \; \frac{\partial H}{\partial r} + \frac{\delta a}{i\omega\mu} \; \frac{1}{r} \; \frac{\partial^2 E}{\partial z \partial \theta} \tag{58}$$

$$H_{(\theta)} = -\frac{\delta}{i\omega\mu} \; \frac{\partial E}{\partial r} + \frac{\delta a}{i\omega\mu} \; \frac{1}{r} \; \frac{\partial^2 H}{\partial z \partial \theta} \tag{59}$$

Now equations (58) and (59) show that, in the absence of θ-dependence, the problem uncouples into TE and TM modes, while the jump-condition requirements (57) prevent this uncoupling in the presence of θ-dependence.

The jump and boundary conditions now lead to the determinantal equation which relates propagation velocity $\widetilde{\gamma}$, to wave frequency ω, and to the plasma frequency ω_p and the configuration r_1/r_2. After some algebraic manipulation this determinantal equation can be put in the following form:

$$T_m = \frac{1}{2} \left(X_m + P Z_m \right) \pm \sqrt{\frac{1}{4} \left(X_m - P Z_m \right)^2 + m^2 \left(\frac{1}{y^2} - \frac{P}{x^2}\right)\left(\frac{1}{y^2} - \frac{1}{x^2}\right)} \tag{60}$$

47

where the parameters used are as follows:

$$y = k_b r_1$$

$$x = k_a r_1$$

$$z = k_a r_2$$

$$P = \cfrac{1}{1 - \cfrac{\omega_p^2 \left(1 - \frac{i\nu}{\omega}\right)}{\omega^2 + \nu^2}}$$

$$k_o = \frac{\omega}{c}$$

$$T_m = \frac{1}{y} \frac{J_m'(y)}{J_m(y)} \qquad ; \qquad Z_m = \frac{1}{x} \left\{ \frac{J_m'(x) - \dfrac{J_m(z)}{Y_m(z)} Y_m'(x)}{J_m(x) - \dfrac{J_m(z)}{Y_m(z)} Y_m(x)} \right\}$$

$$X_m = \frac{1}{x} \left\{ \frac{J_m'(x) - \dfrac{J_m'(z)}{Y_m'(z)} Y_m'(x)}{J_m(x) - \dfrac{J_m'(z)}{Y_m'(z)} Y_m(x)} \right\}$$

(61)

$$k_a^2 = k_o^2 - \bar{\gamma}^2$$

$$k_b^2 = k_o^2 - \bar{\gamma}^2 + \frac{i\omega\omega_p^2}{c_o^2(\nu - i\omega)} = k_a^2 + k_o^2\left(\frac{1}{P} - 1\right)$$

$$k_o^2 = \frac{\omega^2}{c^2}$$

The equation (60) constitutes a transcendental relation between $\omega, \omega_p, \nu, \bar{\gamma}$, and the configuration (r_1/r_2). This equation is currently being solved numerically on the GASL Bendix G-15 computer.

48

4. RESONANT MODES IN PLASMA-FILLED CAVITY

In this section, the effect of an external axial magnetic field is analyzed, assuming a standing wave distribution of the electromagnetic wave inside the wave guide. In this case, we may study the resonant modes of a plasma-filled cavity of length z_0 and radius r_0, under the externally applied magnetic field H_0. The minimum value of the length z_0 of the cavity corresponds to half a wavelength of the standing wave inside the wave guide.

The Y_m solutions must be ruled out from considerations of boundedness at the origin. Thus, for this problem, E is given by

$$E = \left(A\, J_m\left(r\, k_1 \right) + B\, J_m\left(r\, k_2 \right) \right) \sin\frac{\pi z}{z_0}\, e^{i\left(-\omega t + m\theta \right)} \tag{62}$$

The remaining two boundary conditions, from which A and B (the mode shape) and the resonant frequencies are obtained are:

$$E\left(r_0 \right) = 0 \tag{63}$$

and

$$E_{\left(\theta \right)}\left(r_0 \right) = 0 \tag{64}$$

The first, (63), follows simply from (62):

$$A\, J_m\left(r_0 k_1 \right) + B\, J_m\left(r_0 k_2 \right) = 0 \tag{65}$$

The second, (64), requires the use of (26) for E_s, which in turn requires a knowledge of H. Using (42) and (43), H is expressible in terms of E and operators thereupon.

When this process is carried out, and when the vanishing of E itself on the wall $r = r_0$ is accounted for, the second homogeneous equation on A and B becomes:

49

$$A\left[(\gamma a + \delta\beta)\ \frac{im}{r_o}\ \frac{1}{i\omega\mu}\ k_1^2\ J_m\ (r_o\,k_1) + k_1\ J_m'(r_o\,k_1)\ \left(1 - k_2^2\ \frac{\delta a - \gamma\beta}{i\,\omega\,\mu}\right)\right]$$

$$+\ B\left[(\gamma a + \delta\beta)\ \frac{im}{r_o}\ \frac{1}{i\omega\mu}\ k_2^2\ J_m(r_o\,k_2) + k_2\ J_m'(r_o\,k_2)\ \left(1 - k_1^2\ \frac{\delta a - \gamma\beta}{i\,\omega\,\mu}\right)\right] = 0 \qquad (66)$$

Equations (65) and (66) provide the determinantal relation for a nontrivial solution vector (A, B) from which the modal frequencies are computed. It can easily be shown that, for $\omega_H = 0$ (zero applied magnetic field) k_1 and k_2 become equal, invalidating the solution form (62). However, examination of (42) and (43), (noting that β and γ vanish with ω_H) shows that H and E decouple in this case, permitting decomposition into the conventional TM (H= 0) and TE (E= 0) modes. The natural modes and frequencies for this case (when $\nu = 0$) are classical provided ω^2 in the classical problem is replaced by $(\omega^2 - \omega_p^2)$. That is

$$\omega_{(n)}^2 = \omega_{(n)}^2{}_{classical} + \omega_p^2 \qquad (67)$$

for the nth mode.

The determinantal relation, corresponding to equations (65) and (66) is currently being solved numerically in the GASL Bendix G-15 Computer. At a set of values of ω_H, ω_p and geometry r_o/z_o, trial values of frequency ω are inserted until a zero-crossing is obtained for the value of the determinant. Great care must be taken in the interpretation of the solutions so obtained, since some formal solutions exist (vanishing of the determinant) which correspond to trivial fields. Such is the case, for example, when either k_1 or k_2 vanishes; then it is possible to have a trivial field even though the vector (A, B) is nontrivial.

50

CHAPTER V

EXPERIMENTAL FACILITY

1. INTRODUCTION

In this chapter we describe the facility which will be used for the measurement of the electromagnetic properties of a nonuniform plasma. The first part contains a description of the shock tube and the results of calculations concerning the state of the test plasma. The second part contains a description of the test section and the discussion of the electromagnetic measurements.

2. THE SHOCK TUBE

In studies such as the one presently under consideration, where the thermodynamic state of a slug of high purity gas must be accurately known, shock tubes have often been successfully employed (References 1-3) . The shock tube offers several unique advantages over other devices which produce high temperature flows. Some of these advantages are: 1) the state of the gas in the shock tube can be precisely determined from a knowledge of properties of the gas and the velocity of the shock as it traverses the tube; thus it is not necessary to disturb the gas sample with probes in order to determine its state; 2) the purity of the test gas is controllable, as it never makes contact with an electrode or any high temperature surface; and 3) as long as the shock velocity and conditions ahead of the shock are uniform, the gas sample produced will also be uniform, since heat transfer to the tube walls is negligible during the short time involved in any test.

In the current study, all the above-mentioned advantages of the shock tube are needed. Electron density and plasma frequency of air are strong functions of the thermodynamic state and the impurity level of the sample, and both must be accurately known and controlled. Uniform gas samples are needed for the calibration of the microwave equipment.

As discussed in Section 3 of this chapter, it was desired to construct a shock tube to produce a slug of hot air, or plasma, about 18 inches in length and 3 inches in diameter, with equilibrium electron densities n_e between 10^7 and 10^{11} electrons/cc, i.e. plasma frequencies ν_p between 3×10^7 and 3×10^9 c.p.s. Both uniform and nonuniform electron density samples were required, with the nonuniform samples having a known axial electron density gradient.

As a preliminary step in determining the shock tube needed for the study, the equilibrium electron density behind a shock was calculated for various shock Mach numbers M_s in air at room temperature and various pressures. Since it was desired to avoid high pressures in the test section to facilitate the microwave detector installation, it was decided to design the experiment for an initial pressure p_1 of 0.01 atmospheres. This pressure level is easily achieved, and results in a maximum test section pressure (after shock reflection) of 8.5 atmospheres. The results of these electron density calculations, based on data from References 4 and 5, are shown in Figure 1.

In order to produce a significant axial variation of electron density in the test gas, it was thought necessary to create an axial temperature gradient behind the shock moving down the tube, since electron density of a gas is primarily a

52

function of temperature. The most convenient method of creating a temperature gradient behind the incident shock is by varying the temperature in front of the shock. This will cause both the shock velocity and shock Mach number to change as the wave passes through the initial temperature gradient and, by careful selection of the initial shock Mach number, initial temperature, and initial temperature gradient, it should be possible to produce the desired gradient behind the shock.

By means of a simplified analysis, the results of various Mach number, temperature, and temperature gradient combinations have been estimated, and the most promising of these have then been accurately calculated by means of a real gas characteristics program for the Bendix G-15 computer.

The simplified analysis is performed as follows: We choose values of M_{s_i}, T_{1_i} and ΔT_1 or T_{1_f} (for meanings of symbols, see nomenclature list). We assume that hydrogen at room temperature is the driver gas, and air at 0.01 atm. is the driven gas. It is well known that the diaphragm pressure ratio p_4/p_1 is a function of M_s, a_1, and a_4. We can thus compute p_4/p_1 for the a_1 corresponding to T_{1_i}, and for M_{s_i}. This same pressure ratio is then used to compute M_{s_f} assuming a_1 corresponds to T_{1_f}. We now have two different shock Mach numbers which correspond to the two different initial temperatures at the ends of the initial temperature distribution. By using References 4 and 5 we can determine T_{2_i}, T_{2_f}, ρ_{2_i}, ρ_{2_f}, and n_{e_i} and n_{e_f} from these. Although this analysis does not give details of the electron density gradient, it does predict the maximum variation of electron density we can expect in the plasma behind

53

the incident shock. When the results of such an analysis were satisfactory, a detailed one-dimensional unsteady characteristics solution was obtained for the same values of M_{s_i}, T_{1_i}, and T_{1_f}. The computer program was a modified version of the one described in Reference 6.

The results of the preliminary analysis showed that a satisfactory gradient for a typical test case might be established by choosing M_{s_i} = 5.5, T_{1_i} = 450°K, and T_{1_f} = 300°K, with p_1 = 0.01 atm. These numbers were then fed into the Bendix computer in a nondimensional form which specified that the initial temperature in the driven tube decreased linearly with distance along the tube. The length over which the temperature change occurred was arbitrary in the nondimensional coordinates.

From the numerical solution of the problem it was found that the shock slows down as it traverses the region of decreasing initial temperature, but the shock Mach number increases due to the decreasing value of sound speed ahead of the shock. The final shock Mach number was 6.2. It was also found that T_{2_i} = 2570°K, T_{2_f} = 2200°K, n_{e_i} = 1.5×10^9 and n_{e_f} = 3.1×10^7 electrons/cc.

For reasons that will be discussed below, it was thought convenient to make the driven tube 40 feet long, with the test section extending this by several feet. If we heat the tube as shown in Figure 2, with the initial temperature gradient coming between the 35-foot and 40-foot stations, and if we consider the instant when the shock is 43.5 feet from the diaphragm station, i.e. 3.5 feet into the test section, then the plasma temperature and electron density in the test section will be as shown in Figure 3. It can be seen that the resulting

54

electron density gradient falls within the desired range of values.

It should be noted that the above analysis, while based on real gas computations, does not take into account shock velocity nonuniformities due to such phenomena as boundary layer growth and finite diaphragm opening time. Furthermore, no accurate theory exists which can predict these nonuniformities. In an actual test, we plan to avoid the problem of accurate prediction of shock velocity. This will be done by measuring the shock velocity at eight stations along the tube. These measurements, along with a knowledge of the initial temperature distribution in the driven tube, will permit an accurate calculation of the actual electron density gradient behind the shock. The computer will perform these calculations.

In order to correctly calculate electron density using velocity measurements, these measurements must be made with great precision. Analysis has shown that the error in electron density is given by the following relation:

$$\frac{dn_e}{n_e} = 2\left(\frac{\partial \ln n_e}{\partial T}\right)_\rho T_2 \left(\frac{du_s}{u_s}\right) - \left(\frac{\partial \ln n_e}{\partial \rho/\rho_o}\right)_T \frac{\rho_2}{\rho_o}\left(\frac{dT_1}{T_1}\right)$$

where dX/X is defined as the per cent error in the assumed value of X. For our range of interest ($T_2 = 2200 - 3000\,^\circ K$) this becomes:

$$\max\left(\frac{dn_e}{n_e}\right) = \left| 52.8\left(\frac{du_s}{u_s}\right)\right| + \left|0.368\left(\frac{dT_1}{T_1}\right)\right| .$$

Thus, if we can measure u_s with 0.1% accuracy we will still have an error of more than 5% in electron density. The error of a few degrees that we may make in T_1

55

will have little effect on the error in n_e. We plan to accomplish the velocity measurement by using eight pair of ionization probes distributed along the driven tube and test section. Each pair of probes will constitute one velocity measuring station, with the two probes about two feet apart. The ionization behind the shock wave will trigger each probe in turn, and the probes will act as shock time-of-arrival indicators. Special circuits have been designed to measure and record the outputs with the required accuracy (0.2×10^{-6} seconds).

The primary factor which was used to fix the length of the shock tube was the length of the plasma slug required. If ideal gas relations are used, the plasma length per unit length of driven tube is given by $1 - \frac{u_2}{a_1} \frac{1}{M_s}$. This will be reduced due to real gas effects and attenuation. For $5.5 \leq M_s \leq 6$ we estimate real plasma lengths of about 0.08 feet per foot of driven tube. Now, for our test we will require about 3.5 feet of plasma, and thus we have chosen to use a 40-foot driven tube plus a test section about 4 feet long. The driver is 10 feet long. The entire shock tube, including driver section, has a nominal inside diameter of three inches.

The temperature distribution is obtained by winding insulated nichrome wire helically around the driven tube. The wire is heated by passing current through it, and is divided into 15 individually controlled sections which allow the establishment of any desired initial temperature distribution. The entire driven tube is thermally insulated from the surrounding air and supporting stand.

Heat from the tube wall will be conducted to the low-pressure air in the driven tube, and the initial temperature distribution in the air should follow closely that of the tube wall. Convection is not expected to play a major role in the transfer process.

56

Although it was originally thought that our tests would be performed in the GASL shock tunnel, we soon realized that, due to the moderate values of temperature and pressure required, it would be more economical and convenient to construct a new shock tube with relatively thin walls. Much less power is required to heat this new tube, which is made of stainless steel pipe, to the desired initial temperature distribution, and the cost of building the tube is considerably less than that of extending the shock tunnel tube to a length of 40 feet.

In the body of shock tube literature available no reference is to be found of any facility using this type of differential preheating of the driven gas. Thus we believe we have developed a unique and versatile research tool.

From the values of shock Mach number and initial pressure to be used, we can calculate the hydrogen pressure needed in the driver. This is of the order of 10 atmospheres; a nonmetallic diaphragm is used to contain this. In order to control the shock Mach number produced we will charge the driver and driven tubes to the desired pressures using a diaphragm which will not burst at these pressures. Then a wire in contact with the diaphragm will be heated electrically, and thus weaken the diaphragm material until it bursts. The amount of heating required to produce a good burst should be small. The diaphragm is thermally insulated from the heated driven tube by phenolic rings.

In an attempt to estimate the effects of boundary layer on the flow in the shock tube, the distance behind the shock at which transition occurs has been calculated. Assuming a transition Reynolds number of 6×10^{6} based on the distance a particle has moved after the shock has passed over it, we found that transition occurs 24 inches behind the shock in the test section. Thus we will have about two feet of laminar boundary layer.

57

The electron density profile in the laminar boundary layer has been computed, using data from Reference 7 with the equilibrium value for plasma temperature. The results of this calculation are shown in Figure 4. We see that a Mach 6 shock, moving into air at $300^\circ K$ and 0.01 atmospheres (approximately the conditions existing in the test section), produces a boundary layer in which, two feet behind the shock, the electron density has decreased 10% from free stream at 0.18 inches from the tube wall. We can define a core area, within which the electron density is no more than 10% from its free stream value, and the ratio of core area to total area will vary as in Figure 5.

In the course of our tests, an antenna at the end of the test section will be radiating electromagnetic waves upstream, through the oncoming shock, and into the hot plasma behind the shock. To prevent this radiation from continuing upstream, reflecting off the end of the driver, and coming back downstream to interfere with the tests, we have designed an electromagnetic trap which, when installed in the tube, will transform the test section into an electromagnetic cavity. This trap will consist of one or more metallic ribbons stretched across the tube between the test section and the driven tube. The ribbons will be 0.001 inches thick with a chord of about 0.25 inches, and will be in tension to prevent fluttering. The flow in the test section is not expected to be affected, since the ribbons will be several inches upstream of the region of interest.

58

3. EXPERIMENTAL INVESTIGATION OF THE PLASMA PROPERTIES

The preceding section discussed the aerodynamic requirements and properties of the GASL shock tube built for this experiment. In this section, we discuss the experimental facility to determine the electromagnetic properties of a nonuniform plasma. The use of a shock tube to generate a plasma is highly advantageous for the reasons previously mentioned. However, using the plasma region behind the shock wave imposes severe requirements on the experimental technique to measure the electromagnetic properties of the ionized slug. The primary difficulty is due to the short duration that the plasma region is properly located in the electromagnetic test section. For a uniform plasma such as that generated in a conventional shock tube, the running times are on the order of 100 μsec. However, for an axially nonuniform plasma, it is clear that the electromagnetic properties are constantly changing while the slug is passing through the test section. A number of interesting phenomena may occur as the slug enters the testing region. Such phenomena may have very short transients. For these reasons, it was deemed necessary that the detection system have a high time resolution ability.

The second condition to be satisfied by the ionized gas is given by the maximum value of the electron density at which the electromagnetic wave can propagate through the plasma. A suitable compromise between mechanical feasibility of the shock tube and a convenient frequency of the electromagnetic wave suggested a tube diameter of 2.94 inches. This diameter is maintained for both the driven and test sections. In the cylindrical wave guide corresponding to the test section, the TE_{11} mode was selected for the electromagnetic wave.

59

This mode allows the use of a minimum frequency in the range of 3×10^9 **cycles** per sec. On the other hand, this frequency is lower than the cut-off frequency of the TM_{01} propagation mode. The frequency of the electromagnetic wave determines the maximum value of the electron density in the ionized gas which corresponds to approximately 10^{11} electrons per **cc.**

The minimum electron concentration is determined by the minimum detectable signal from the electromagnetic probes. With the present technique, it is probable that the minimum detectable electron density is approximately 10^7 electrons/cc.

Since it is the purpose of this investigation to study the properties of nonuniform plasma, the electron density in the extreme case should be rapidly changing in a distance comparable to one wavelength. By establishing a temperature gradient in the tube as discussed in the previous section, an electron gradient as strong as one order of magnitude every two wavelengths can be realized.

Another difficulty in using the plasma generated behind the shock wave is that the electron density is not radially uniform. This lack of uniformity leads to an average electron concentration which is lower than the electron density at the axis of the tube. Since the electrodynamic properties of the plasma can only be conveniently measured by considering the whole tube as a waveguide uniformly filled with a dielectric medium, the radial plasma nonuniformity must be minimized. Since the radial plasma nonuniformity is closely related to the aerodynamic boundary layer, great care was taken in the design and construction of all parts of this facility to minimize the boundary layer growth as the shock wave proceeds down the tube. The effect of the radial nonuniform plasma

60

distribution is being analyzed from a theoretical point of view as contained in Chapter III. The aforementioned conditions determine the basic design considerations for this facility. The major elements of this design are discussed below.

In Figure 7, the end of the driven part of the shock tube is shown. A microwave cavity is formed between the ribbon section and the tuning slug in the antenna section. The microwave power in the range of 3 kilomegacycles is fed to the antenna which is stretched across the tube approximately $1/4$ wavelength from the tuning slug. The complete microwave system is outlined in block form in Figure 6.

The detection assembly is located three wavelengths from the antenna section to avoid the effects of the attached field in the antenna region. Ten detectors are mounted at quarter wavelength intervals for the median waveguide wavelength. Each detector is a modified crystal with an individually-adjustable capacitive coupling. The probe is mounted flush with the wall of the tube to minimize boundary layer growth. The coupling between a probe and the waveguide must be kept at a minimum value to avoid a large perturbation of the field distribution in the waveguide.

In order to record data from the detectors, special ultra high gain amplifiers are needed. Since it is desirable to observe the short transient effects as the shock passes, these amplifiers were required to have a band pass of 7 megacycles. Since the data of each detector must be recorded independently, it was deemed best that individual oscilloscopes and cameras be employed for each detector. Since no commercially available scope with the desired band pass and sensitivity was available within reasonable cost, the ten scope units were designed and

61

built by the GASL facility. The instrument design incorporates a precision attenuator and a variable bandpass switch to accurately determine the short and medium drift in the microwave generator. All of the scopes are driven with a common sweep and trigger source. The specification on each scope is as follows:

Deflection sensitivity from 100 μv/cm to 1 v/cm in calibrated steps.

Rise time - .050 μ sec.

Bandpass - 1/2 to 7 mc adjustable.

Noise - input open circuited - 20 μv RMS.

- input short circuited - 10 μv RMS.

It should be noted that each detector is AC coupled to the amplifiers so that only the change in microwave signal is displayed on the scope.

In Figure 8 a field distribution is shown typical of that encountered if the plasma has an axial gradient. Note that the wavelength has shifted and that the signal is partially attenuated.

For comparison, the field distribution for the waveguide without plasma is superimposed. The recorded data during the plasma flow will determine the instantaneous departure of the field distribution with respect to the stationary distribution prior to each experiment. This data is recorded on a continuous time basis during the running time of the tube. Hence, for each detector, a history of the difference between the zero plasma case and the incident plasma is made. By comparing the ten histories thus recorded, the field distribution and hence the wavelength and attenuation can be determined for all times during the test. A particularly interesting situation may be found when the electron

density increases behind the shock reaching the critical value which corresponds to a plasma frequency equal to the angular frequency of the electromagnetic wave. The position in the ionized layer of this critical density corresponds to the transition from the propagation region to a region of complete attenuation of the electromagnetic wave. The passage of this transition plane by the position of a detector leads to a drastic change in the time-dependent signal obtained by the detector. We point out that it is of major interest to analyze the correlation between the theoretical calculation and the experimental results across this transition region. This is due to the fact that the position of this transition region in the plasma may be strongly affected by even a small departure of the actual electromagnetic properties of the plasma from the theoretical model.

At the present date, all of the mechanical work on the shock tube has been completed. In addition, all of the microwave equipment and the test section has been finished. The data recording system composed of the detectors, scope amplifiers, scopes and sweep source are complete except for calibration. In like manner, the heating and control system for establishing a variable gradient in the tube is finished. The only remaining pretest work on the facility is principally a careful calibration of all components. It is expected that preliminary test runs will be started shortly.

REFERENCES - CHAPTER V

1. Daiber, J.W., and Glick, H.S., Plasma Studies in a Shock Tube, Cornell Aeronautical Laboratory Report No. AF-1441-A-4, July 1961.

2. Lin, S.C., Resler, E.L., and Kantrowitz, A., Electrical Conductivity of Highly Ionized Argon Produced by Shock Waves, Jl. Appl. Phys., **Vol.** 26, p. 95, 1955

3. Hertzberg, A., The Application of the Shock Tube to the Study of High Temperature Phenomena in Gases, Appl. Mech. Rev., **Vol.** 9, p. 505, 1956.

4. Feldman, S., Hypersonic Gas Dynamic Charts for Equilibrium Air, Avco Research Laboratory, 1957.

5. Feldman, S., Trails of Axi-Symmetric Hypersonic Blunt Bodies Flying Through the Atmosphere, Avco Research Laboratory Report No. 82, December 1959.

6. Moretti, G., and Tamagno, J., Study of a Shock Tube Attachment to Simulate the Shock Layer Past an ICBM Flying at Very High Altitudes, General Applied Science Laboratories, Inc., Technical Report No. 189, October 1960.

7. Mirels, H., Laminar Boundary Layer Behind Shock Advancing Into Stationary Fluid, NACA TN 3401, March 1955.

SYMBOLS - CHAPTER V

a   speed of sound

A   tube cross section area

M_s shock Mach number : u_s/a_1

n_e electron density

p   pressure

T   temperature

ΔT_1 $T_{1_i} - T_{1_f}$

u   velocity

X   any variable

x   axial distance, either from diaphragm or behind shock

y   normal distance from wall

ν_p plasma frequency

ρ density

Subscripts

o   reference conditions $\left(\begin{array}{l} T_o = 273.16^{\circ}K \\ p_1 = 1 \text{ atm}, \rho_o = 1.288 \times 10^{-3} \text{ gm/cc} \end{array} \right)$

1   initial conditions in driven tube

2   conditions in plasma behind shock wave

4   initial conditions in driver tube

i   conditions at diaphragm end of region of interest

f   conditions at test section end of region of interest

s   pertaining to shock wave
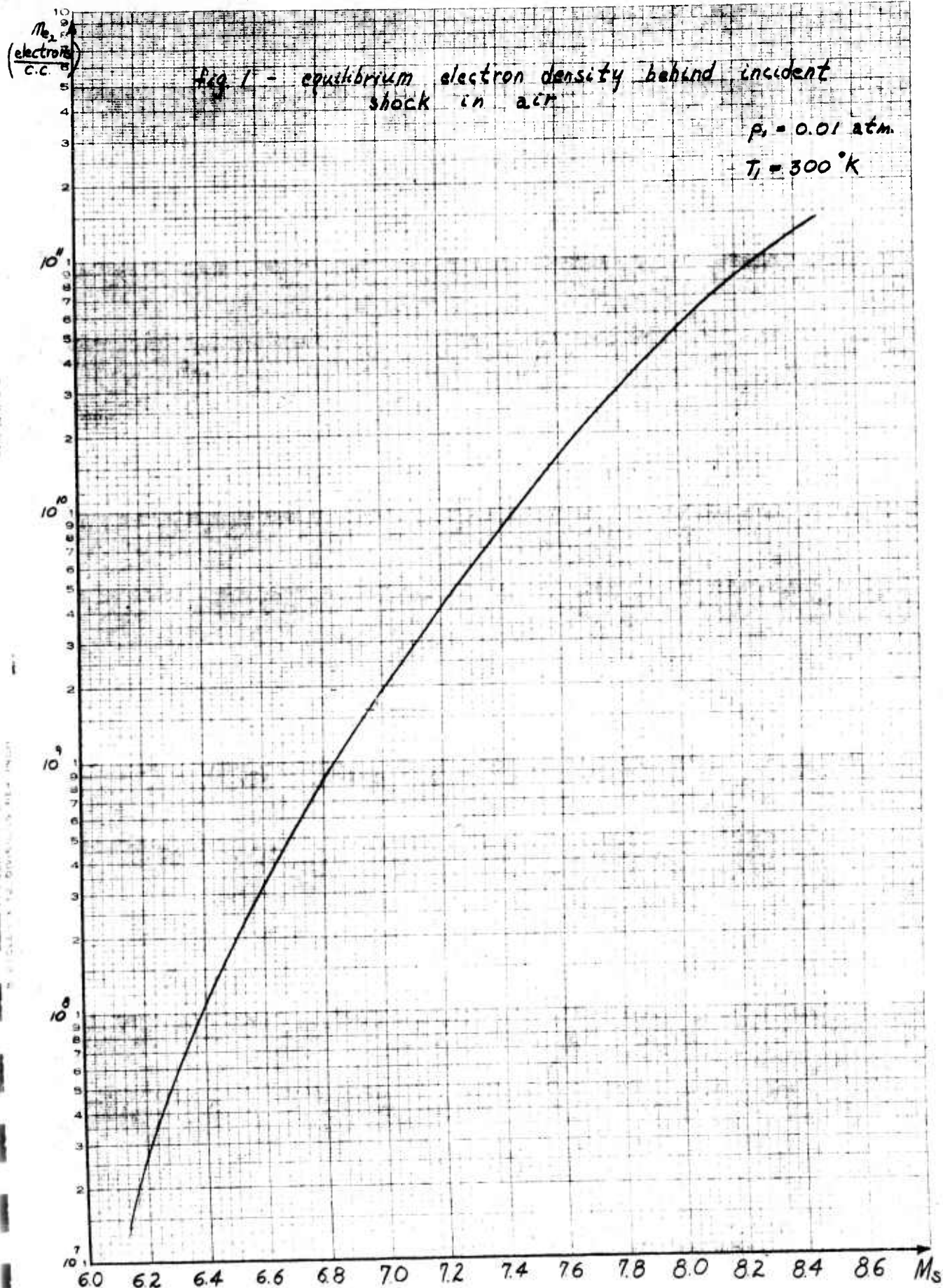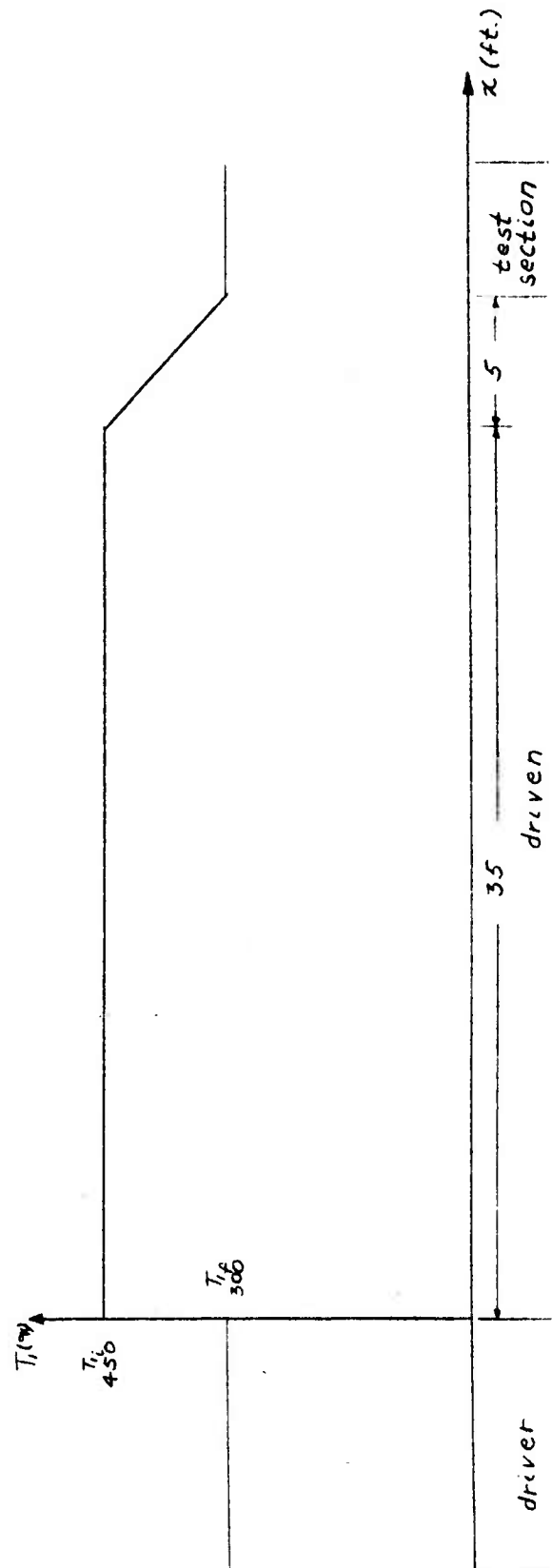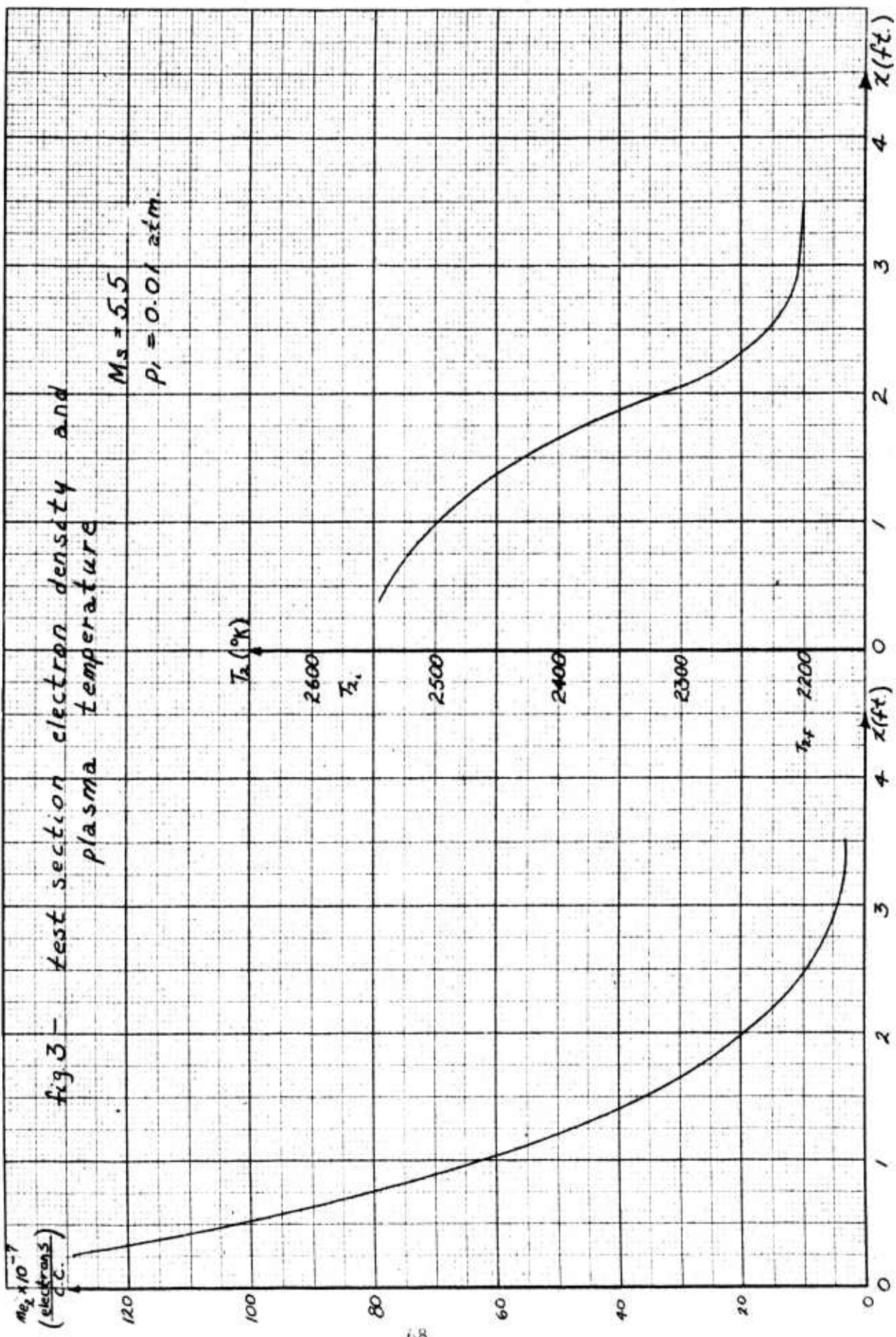
Fig 1 - equilibrium electron density behind incident shock in air

$p_1 = 0.01$ atm.

$T_1 = 300°K$

fig. 2 - initial temperature distribution

fig. 3 - test section electron density and plasma temperature

$M_s = 5.5$

$\rho_1 = 0.01$ atm.

fig 4 - electron density profile behind Mach 6 shock in air

$T_1 = 300\ °K$ $p_1 = 0.01$ atm.

$y =$ inches from tube wall
$x =$ inches behind shock

fig 5 - fraction of tube area where electron density is within 10% of free stream value

$Ms = 6$; $T_1 = 300\ °K$; $p_1 = 0.01$ atm.

69
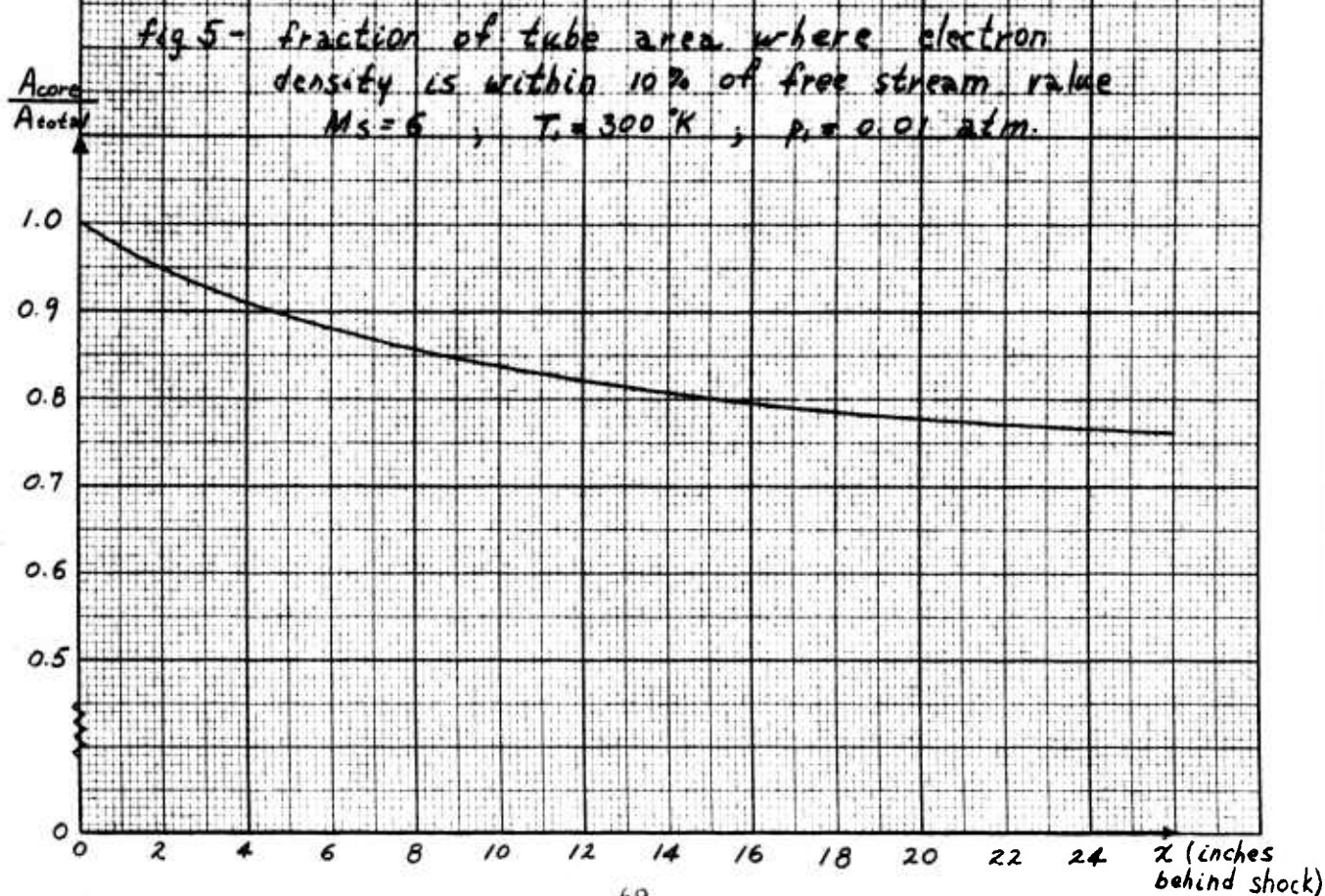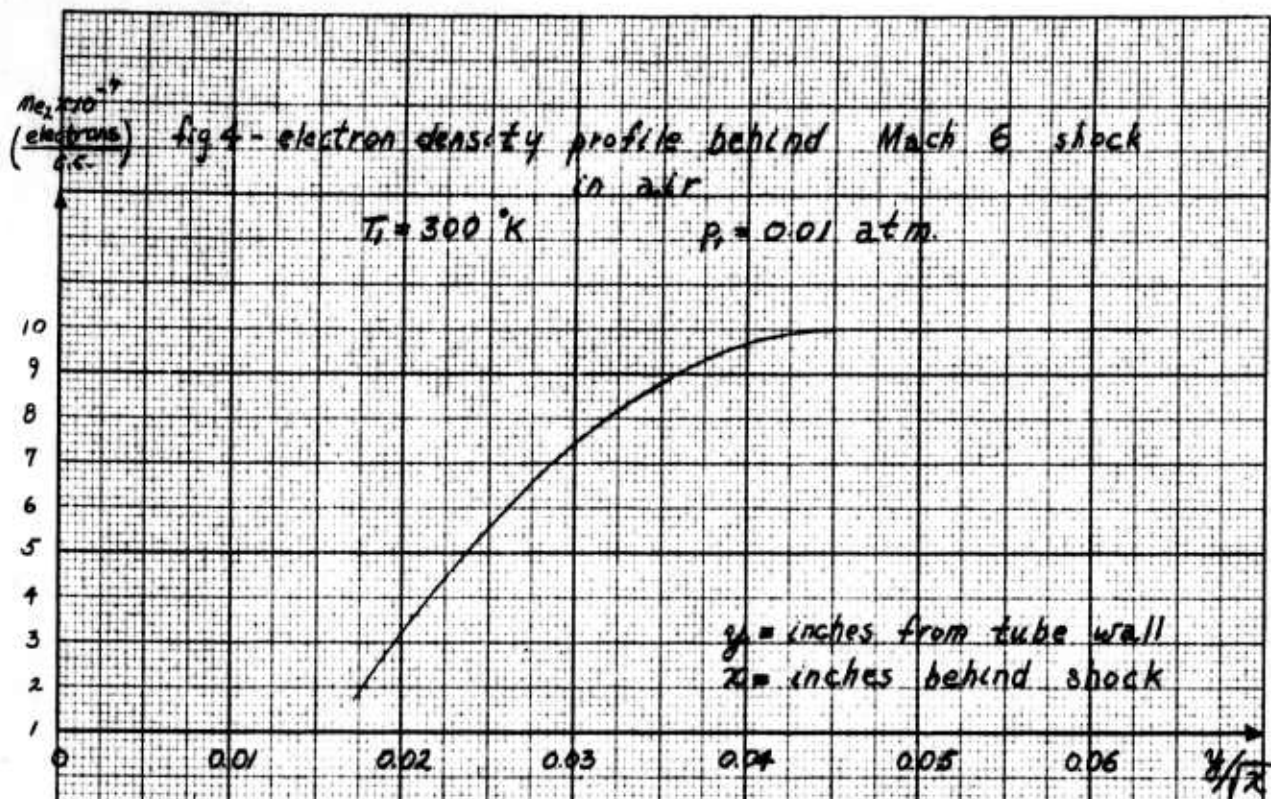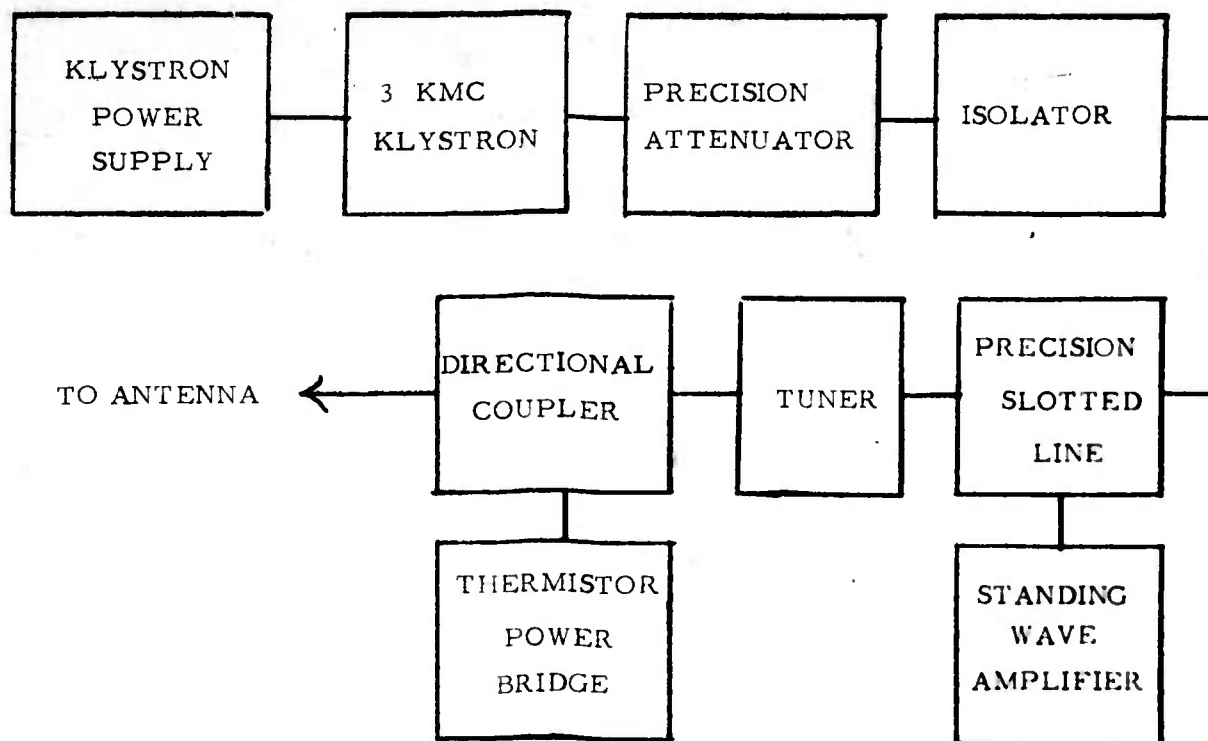
FIGURE 6. MICROWAVE SYSTEM
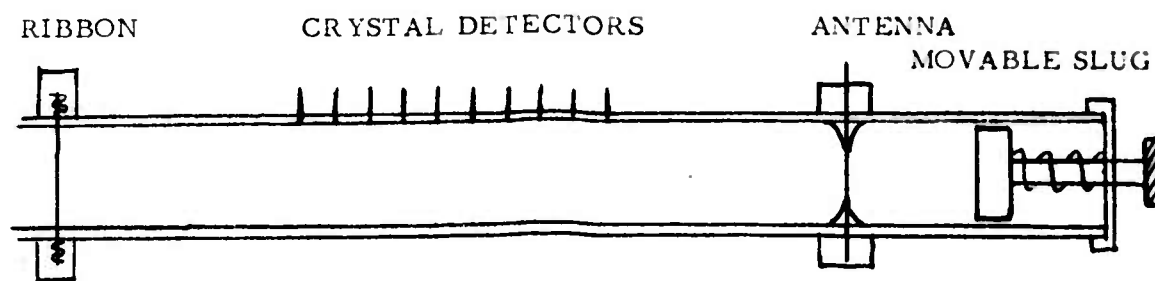
FIGURE 7. LONGITUDINAL CROSS SECTION OF TEST CHAMBER
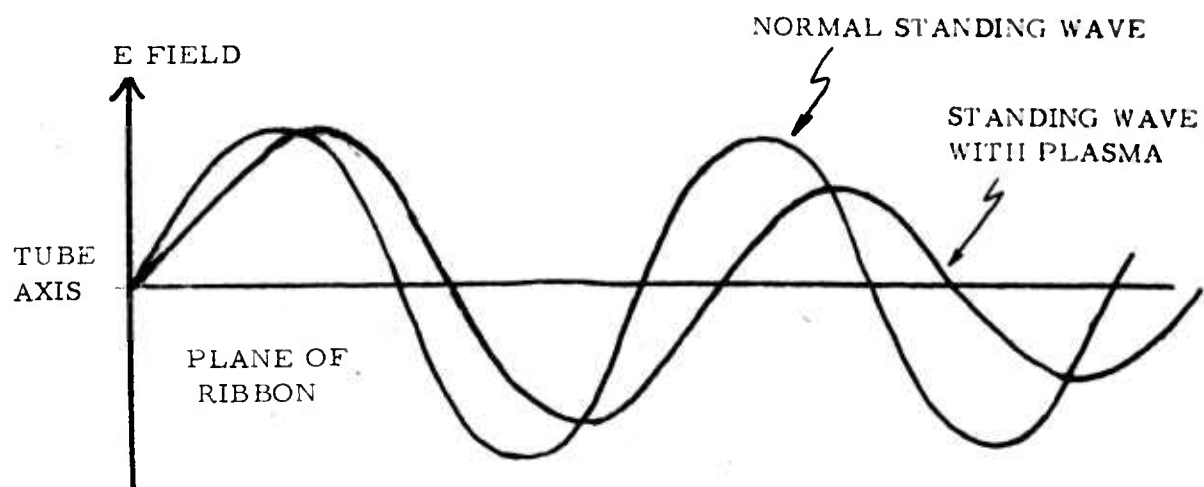
FIGURE 8. TYPICAL STANDING WAVE PATTERNS

70